NeuroImage 300 (2024) 120870

Contents lists available at ScienceDirect

NeuroImage

journal homepage: www.elsevier.com/locate/ynimg

Neuro-cognitive effects of degraded visibility on illusory body ownership

Gustavo S.P. Pamplona [a,b,c], Amedeo Giussani [a], Lena Salzmann [b], Philipp Staempfli [d], Stefan Schneller [b], Roger Gassert [b], Silvio Ionta [a,*]

[a] Sensory-Motor Laboratory (SeMoLa), Jules-Gonin Eye Hospital/Fondation Asile des Aveugles, Department of Ophthalmology/University of Lausanne, Lausanne, Switzerland
[b] Rehabilitation Engineering Laboratory (RELab), Department of Health Sciences and Technology, ETH Zurich, Zurich, Switzerland
[c] Department of Child and Adolescent Psychiatry and Psychotherapy, University Hospital of Psychiatry Zurich, University of Zurich, Zurich, Switzerland
[d] Department of Adult Psychiatry and Psychotherapy, Psychiatric University Clinic Zurich and University of Zurich, Zurich, Switzerland

ARTICLE INFO

Keywords:
Rubber hand illusion
Brain
Fmri
Vicarious pain
Vision
Touch

ABSTRACT

Based on visuo-tactile stimulation, the rubber hand illusion induces a sense of ownership for a dummy hand. Manipulating the visibility of the dummy hand during the stimulation influences cognitive aspects of the illusion, suggesting that the related brain activity may be influenced too. To test this, we analyzed brain activity (fMRI), subjective ratings, and skin conductance from 45 neurotypical participants undergoing a modified rubber hand illusion protocol where we manipulated the visibility (high, medium, and low) of a virtual hand, not the brush (virtual hand illusion; VHI). To further investigate the impact of visibility manipulations on VHI-related secondary effects (i.e. vicarious somatosensation), we recorded brain activity and skin conductance during a vicarious pain protocol (observation of painful stimulations of the virtual hand) that occurred after the VHI procedure. Results showed that, during both the VHI and vicarious pain periods, the activity of distinct visual, somatosensory, and motor brain regions was modulated by (i) visibility manipulations, (ii) coherence between visual and tactile stimulation, and (iii) time of visuo-tactile stimulation. Accordingly, embodiment-related subjective ratings of the perceived illusion were specifically influenced by visibility manipulations. These findings suggest that visibility modifications can impact the neural and cognitive effects of illusory body ownership, in that when visibility decreases the illusion is perceived as weaker and the brain activity in visual, motor, and somatosensory regions is overall lower. We interpret this evidence as a sign of the weight of vision on embodiment processes, in that the cortical and subjective aspects of illusory body ownership are weakened by a degradation of visual input during the induction of the illusion.

1. Introduction

Feeling that our own body belongs to ourselves (body ownership) is a fundamental aspect of self-consciousness, enabling us to properly interact with the environment and other people. In experimental setups, body ownership can be manipulated through the well-known rubber hand illusion (RHI) protocol (Botvinick and Cohen, 1998). If participants' hidden hand is stroked in spatiotemporal synchrony with the stroking performed on a visible dummy hand, most participants report feelings of owning the dummy hand. Broadly speaking, this illusory body ownership results from the relative dominance of vision (viewing the dummy hand being stroked) over touch (feeling one's own hand being stroked). The brain regions typically activated by the RHI are involved in visual and tactile processing (visual and somatosensory cortices), multisensory integration (parietal lobe), and motor control (motor, premotor, and supplementary motor regions) (Garbarini et al., 2020; Golaszewski et al., 2021; Serino et al., 2013; Tsakiris, 2010). In addition, the neuro-cognitive responses to the RHI are not limited to only RHI-specific measures, but rather spread over different domains. In fact, if a threatful event occurs to the dummy hand after the RHI procedure (e.g. the dummy hand is pricked by a syringe needle), participants react to that threat, showing vicarious somatosensory biases for the dummy hand and the activation of the insular and anterior cingulate cortices (Ehrsson et al., 2007a; Pamplona et al., 2022c). Furthermore, varying the procedural parameters of the RHI (tactile and visual inputs), it is possible to modulate the experienced illusory body ownership and the associated brain activity. In fact, in line with the impact of visual manipulations on body-related visuomotor cognition (Giovaola et al.,

* Corresponding author.
E-mail address: ionta.silvio@gmail.com (S. Ionta).

https://doi.org/10.1016/j.neuroimage.2024.120870
Received 10 July 2024; Received in revised form 18 September 2024; Accepted 24 September 2024
Available online 28 September 2024

2022; Rotach et al., 2024), (i) maneuvering the visual aspects of the RHI can influence both subjective ratings (Pamplona et al., 2022a) and objective measurements (Tsakiris et al., 2010), (ii) the RHI is disrupted if the visual aspects are delayed with respect to tactile and motor ones (Lesur et al., 2020), and (iii) progressively less human-like visual setups decrease the strength of the RHI (D'Alonzo et al., 2019). This pattern is confirmed by evidence that a reduced sense of illusory ownership (Martini et al., 2015; Matsumuro et al., 2022; Okumura et al., 2020) and a reduced peripheral response (analgesia) (Matamala-Gomez et al., 2019) are observed even when visibility degradation affects the dummy hand only (not the entire visual field). Notably, these latter studies investigated the role of the visibility of the dummy hand only by manipulating its transparency. This means that in different experimental conditions the dummy hand was clearly visible or progressively more transparent. In this approach, the visual parameters (brightness, contrast, color, saturation, edges, etc.) differ between experimental conditions, possibly inducing, for instance, stronger activity in the visual cortex for conditions with higher versus lower values for visual parameters. Thus, transparency manipulations do not control for the visual parameters across conditions, possibly complicating the interpretation of neural activity modulations associated with visibility manipulations in the context of illusory ownership. It may be difficult to disentangle whether the observed effects must be attributed to the changes in visual parameters due to transparency manipulations or to illusion-related dynamics.

In sum, cognitive and physiological evidence suggests that changes in visual input may influence the activity of brain regions involved in body ownership. However, to the best of our knowledge, the influence of differential visual input on brain responses to RHI has not yet been investigated. To fill this gap, the present study combined brain imaging (functional magnetic resonance imaging – fMRI), video editing, and robotics to investigate whether and how changes in the visibility of only the dummy (virtual) hand influence illusory body ownership, associated brain activity, and peripherally measured arousal (skin conductance response – SCR). In particular, while recording fMRI and SCR, a robotic system compatible with magnetic resonance (MR) delivered precise and reproducible tactile stimulation to the participants' hand (tactile stroking) while, at the same time, pre-recorded video clips of a human hand being stroked were shown (visual stroking). These video clips were edited to modify the level of visibility of only the virtual hand (not the stroking object), while keeping all the visual parameters the same among experimental conditions. After this visuo-tactile stimulation period, participants were shown videos of the virtual hand being pricked with a syringe needle. Subjective ratings of the perceived ownership of the virtual hand were recorded for each trial. Finally, we investigated the widely reported (Botvinick and Cohen, 1998; Fuchs et al., 2016; Gallagher et al., 2021; Riemer et al., 2019; Rohde et al., 2011; Tsakiris and Haggard, 2005) but yet poorly understood (Limanowski et al., 2014b) temporal changes in brain responses associated with illusory body ownership.

2. Materials and methods

2.1. Participants

A total of 54 neurotypical, normal and corrected-to-normal sighted, right-handed adults were recruited to participate in the study, which consisted of one experimental session. The data from the first 5 of these participants (25.8 ± 2.0 years old, age range 24.2–28.2 years, 2 female participants) were used as pilot to determine the definitive sample size based on a power analysis (as described in Section 2.4.1). These 5 datasets were not included in the final data analyses. The power analysis indicated 45 datasets as the ideal sample size. During data recording, 4 datasets had to be discarded due to technical issues. Therefore, after the power analysis, a total of 49 participants were recorded, but the definitive sample comprised 45 participants (26.9 ± 4.5 years old, age range 21.6–40.6 years, 23 female participants), as indicated by the power analysis. These datasets were included in the following analyses. Female and male participants were equivalent in age (Wilcoxon test: $p = 0.24$). All participants gave informed consent and were screened for MR compatibility using an MR safety form. Exclusion criteria at recruitment were: significant left-handedness [cut-off point < 60, as determined by the Edinburgh Handedness Inventory (Oldfield, 1971)]; visual impairment of more than ±6 diopters not correctable with contact lenses (the lenses integrated into the goggles allowed visual correction within this range); contraindications for MR procedures; history of neurological, psychiatric, or cardiovascular disorders; claustrophobia; use of alcohol or other illicit drugs before/during the experiment; pregnancy or lactation; non-compliance with experimental procedures. The study was conducted in accordance with the Declaration of Helsinki (2013) and approved by the local Ethics Committee (KEK 2021–00,562).

2.2. Experimental procedures

2.2.1. Setup

Prior to the experiment, participants were instructed to remain still in the scanner with their eyes open and to breathe regularly. We then verbally explained the experimental timeline (Fig. 1) to the participants before they entered the MR room. During instructions, participants watched an example of the video showing the virtual hand being stroked by a brush (see Section 2.2.3). They were instructed that during the experiment they would have to click a button as soon as they perceived that they owned the virtual hand. The statements for subjectively rating the strength of the perceived illusion were also previously read and explained to them during instructions (see Section 2.2.5).

Next, participants entered the MR room and lay supine on the scanner table. Participants were provided with foam earbuds for hearing protection and headphones for eventual communication. Typically, the RHI is performed on the non-dominant hand (Coppi et al., 2024; Magnani et al., 2024; Moffatt et al., 2024). Therefore, our participants put their left hand on an ergonomic plastic support under which the robot was placed (Fig. 1). Participants' hand was in a prone position, the same position and setup of the virtual hand shown later in the videos, and attached to the plastic support by an armband. This ensured that the participant's hand remained in the same position throughout the experiment. To ensure equivalent tactile stimulation (pressure) for each participant, the height of the robot's manipulandum holding the foam brush was adapted to the thickness of each participant's finger. This was a way to keep the same distance between the foam brush and the participant's hand (and thus the friction of the brush on the skin) for all participants. Participants' right hand was placed on the response pad used to indicate the illusion perception onset and to complete illusion-related subjective ratings. Prior to the start of the experiment, participants were asked to confirm that they felt the foam brush on their index finger. Finally, MR-compatible goggles (Resonance Technology Inc., CA, USA) were placed in front of the eyes of the participants, who were asked to adjust the visual focus to obtain a clear dual-view image covering the entire visual field. To measure skin conductance throughout the functional acquisition, two electrodes were placed on the distal parts of the thumb and middle finger of the left hand, facing the fingertips. A conductive gel (Ten20®) was used at the interface between the fingertip and the electrode.

2.2.2. Overall procedure

The experimental session consisted of four runs, each run composed of six blocks, each block consisting of single trials of visuo-tactile stimulation and vicarious pain, followed by the presentation of a fixation cross and three subjective ratings (Fig. 1). During the visuo-tactile stimulation (virtual hand illusion; VHI) tactile stimulation was delivered by the robot's foam brush to the participant's left index finger, and visual stimulation was presented through goggles showing a left virtual hand from the perspective that participants would have had if they were

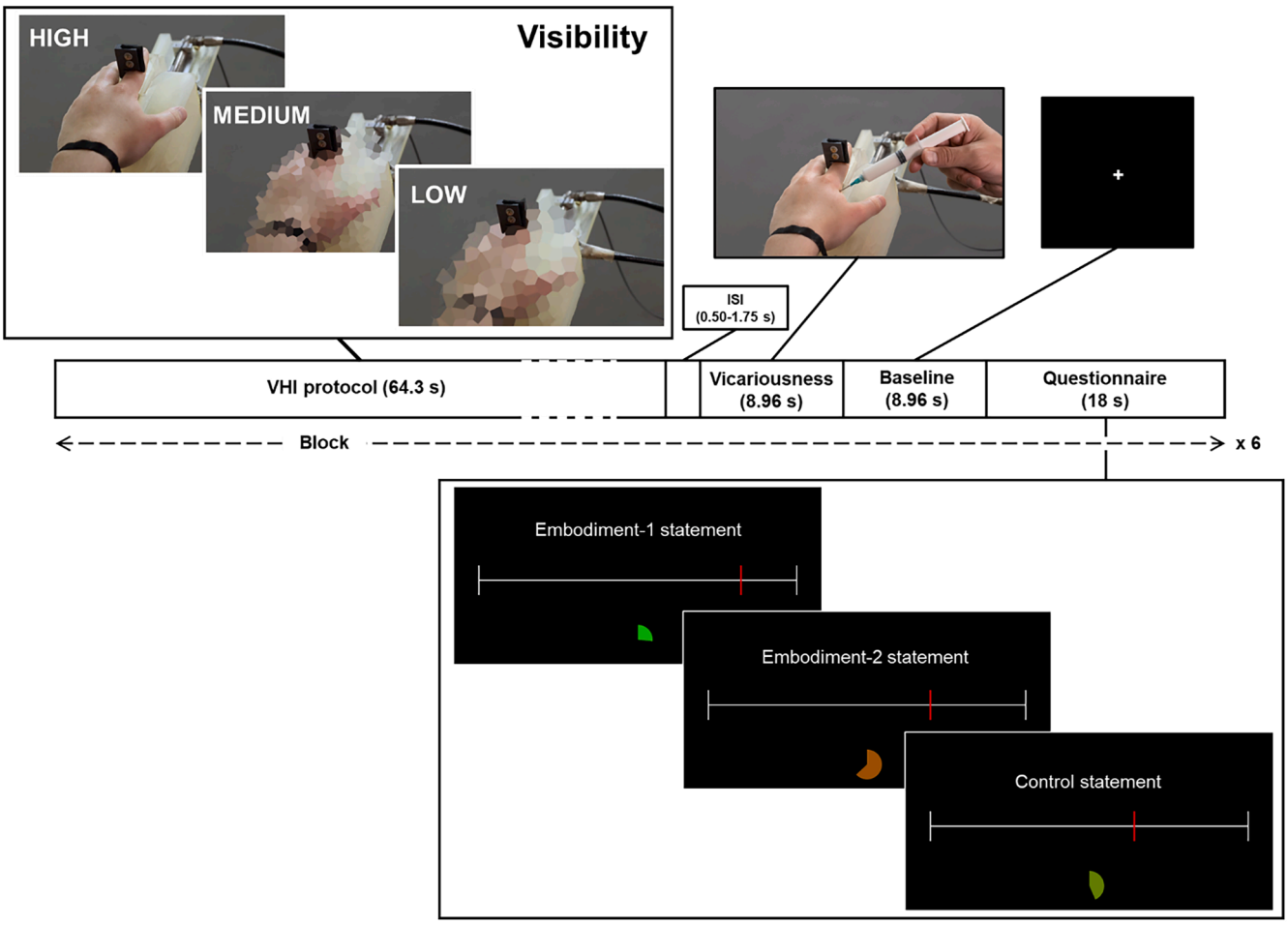

Fig. 1. Timeline of an experimental block. The block started with the visuo-tactile stimulation (VHI protocol): participants' left hand was stroked by a foam attached to the robot manipulandum (tactile stroking) while they watched a video of a human left hand (virtual hand) being stroked by a robot (visual stroking). The tactile and visual stroking could be synchronous or asynchronous. The virtual hand was shown in either high, medium, or low visibility. During the inter-stimulus interval (ISI), participants observed a static image of the virtual hand in high visibility. Immediately after, during the vicarious pain phase (Vicariousness), participants observed the virtual hand being pricked by a needlestick. Then a fixation cross was shown (Baseline), followed by the period of subjective ratings. The experimental block was repeated six times in one run. The durations of each element are shown in seconds.

looking down at their own hand (first-person perspective). In the video, the virtual hand was stroked by the robot's foam brush at the same location where the robot stroked the participant's index finger, for approximately 1 min. The spatiotemporal profiles of the tactile and visual stroking could be either synchronous or asynchronous. During the visuo-tactile stimulation, participants were asked to immediately press a button if they perceived the illusion. Next, participants underwent the vicarious pain protocol, in which the virtual hand was approached and pricked by a syringe needle. During this period, participants were required to only watch the videos. A fixation cross was then presented, followed by the subjective rating of three VHI-related statements.

The visuo-tactile stimulation period varied in terms of visibility of the virtual hand (high, medium, and low visibility) and visuo-tactile profiles (synchronous, asynchronous). The combination of three visibility levels and two visuo-tactile profiles resulted in six possible combinations. Due to the long duration of visuo-tactile stimulation required to induce illusory ownership, each combination was presented only once in each run. The order in which the combinations were presented was randomized for each run and participant. The experimental session lasted approximately 1 h. All items presented were designed with custom code written in MATLAB (The MathWorks, Natick, MA, USA) and Psychtoolbox (http://psychtoolbox.org), and run on a dedicated Windows presentation laptop. The experimental runs were triggered to the fMRI acquisition via a USB port.

2.2.3. *Visuo-tactile stimulation*

The first element of each block was the visuo-tactile stimulation, which lasted 64.3 s (Fig. 1). During this period, participants' left index finger was stroked by the robotic device (tactile stroking) while they simultaneously watched videos of a left Caucasian human hand (virtual hand) being stroked on the index finger by the same robot (visual stroking). The virtual hand was presented from a first-person perspective and was gender-matched to each participant.

2.2.3.1. Tactile stimulation. To provide the tactile stroking, we used a robotic system consisting of a non-MR-compatible master part, placed in the MR control room, and an MR-compatible interface, driven by the master and placed in the MR room (Gassert et al., 2006; Ionta et al., 2011). These two robotic structures were connected by a hydrostatic transmission that passed through an opening between the rooms. The laptop sent predetermined trajectory profiles (see below) to a dedicated desktop computer, equipped with LabVIEW (Laboratory Virtual Instrument Engineering Workbench, National Instruments) and a data acquisition card (PCI 6221, National Instruments) via a User Datagram Protocol connection and an Ethernet cable. The master part of the robot was controlled by custom code written in LabVIEW. The robot-controlling desktop computer sent the commands of a proportional-integral-derivative controller, to the master part of the robot, which moved a piston with an electromagnetic actuators and an

angular encoder to the desired position. Thus, the hydrostatic transmission allowed the manipulandum of the compatible robot interface to move according to the predefined trajectory. The MR-compatible robot interface was mounted on the scanner table, to the left side of the participants, tilted vertically at approximately 30° so that the participants' left hand was just below their chest, next to their left hip, in a location that could simulate direct vision of the virtual hand. A piece of foam was attached to the manipulandum for stroking (foam brush) and its height relative to the participant's finger was designed to provide gentle tactile stimulation to the participant (Fig. 1). The robot interface provided one-dimensional strokes on the dorsal surface of the participants' left index finger, based on previous evidence that the non-dominant hand is more sensitive to the RHI (Reinersmann et al., 2013; Riemer et al., 2019). Only one finger was stroked in the visuo-tactile stimulation, in line with previous related experiments (Bekrater-Bodmann et al., 2014; Kammers et al., 2009; Riemer et al., 2013). To correct for any minor misalignment or drift, the height of the foam brush and the displacement of the manipulandum were checked and, if necessary, readjusted between runs.

We predetermined two trajectories of tactile stroking, each consisting of sinusoidal, full-length, and short-length robot's displacements. With respect to the total number of displacements, the sinusoidal ones corresponded to 20 %, the full-length ones to the 20 %, and the short-length ones to the 60 %. The maximum velocity of each of these displacements was approximately 3 cm/s, which is known to induce higher subjective and objective levels of ownership and pleasantness (Riemer et al., 2019). These displacements were designed to be randomized and with unpredictable onsets, which is thought to induce heightened levels of illusory ownership (Riemer et al., 2019). Both trajectories began and ended with sinusoidal displacements, but in opposite directions relative to each other. The correlation between the trajectories was minimized iteratively as follows. First, the displacement onsets, directions, and intervals were randomly assigned to keep the same number and type of displacements for both trajectories. Then, the trajectories were spatially smoothed, and we calculated the Pearson correlation between the two trajectories. The procedure was repeated until the absolute correlation value between the trajectories was lower than a predefined value (0.003).

2.2.3.2. Visual stimulation. In line with previous work (Bekrater-Bodmann et al., 2014; Gentile et al., 2015), the visual stroking was provided to participants through video clips of an adult female/-male left human hand, gender-matched for each participant, from a first-person perspective, and being stroked on the index finger by the same robotic device used to the tactile stroking (Fig. 1). Importantly, these videos were edited to modulate the visibility of only the virtual hand (not the rest of the scene, i.e. the stroking foam brush). This approach allowed us to investigate the effects of manipulating the visibility of the dummy hand only, not the stroking tool. The virtual hand's visibility was manipulated using the 'crystalize' feature in Adobe After Effects 2022 at a resolution of 1920 × 1080 pixels. Two levels of "crystallization" were applied to the videos. The weak level of crystallization corresponded to our medium visibility condition (cell sizes of 32 and 45 pixels for male and female hands, respectively, due to the difference in hand size). The strong level of crystallization corresponded to our low visibility condition (cell sizes of 51 and 70 pixels for male and female hands, respectively). This approach resulted in three levels of visibility for the virtual hand of each gender: high visibility (no crystallization), medium visibility (weak crystallization), low visibility (strong crystallization). The choice to show the virtual hand being stroked by the same robot used to provide the tactile stimulation was made in order to (a) increase the chances of participants' identification with the virtual scene, and (b) minimize the induction of neural processes related to the mere observation of actions performed by humans (Ebisch et al., 2008).

2.2.3.3. Visuo-tactile integration. The tactile and visual stroking could be either synchronous or asynchronous. In the synchronous condition (hereafter "sync") the tactile and visual stimulations followed the same trajectories, that is the visual stroking videos showed the virtual hand being stroked in the same parts at the same time with respect to the tactile stroking received by the participant through the robotic foam brush (the robotic movement was synchronized with the frame rate of the video). In the asynchronous condition (hereafter "async") the trajectories of the visual and tactile stroking were different, in that the parts of the participant's finger being touched by the robotic foam brush did not correspond to the parts of the virtual hand being "touched" in the video clips. Asynchronous visuo-tactile stimulation is a common control condition in RHI experiments to induce lower levels of illusory limb ownership while maintaining the same load of visual and tactile elements of the synchronous condition (Armel and Ramachandran, 2003). The combination of the different levels of Visibility (high, medium, low) and visuo-tactile Stimulation (synch, async) resulted in six experimental conditions. During each run, each of these six conditions was presented once during the visuo-tactile stimulation period. The order of conditions was pseudorandomized and counterbalanced for each participant.

2.2.4. Vicarious pain

In the second element of the block, after the visuo-tactile stimulation, the vicarious pain period of the experiment consisted of video clips of a syringe needle approaching and pricking the same gender-matched virtual hand as in the visual stroking videos, shown from the same perspective (Fig. 1). This second phase lasted 8.96 s. A 600-ms black screen was presented between the visuo-tactile stimulation and the vicarious pain periods. Then, the first frame of the vicarious pain video was first displayed statically (i.e., with the virtual hand lying on the robot interface) for a pseudorandomized inter-stimulus interval (ISI) to jitter the interval between stimulations and eliminate temporal correlation in the brain response signal. The ISI ranged from 0.50 to 1.75 s, in steps of 0.25 s (i.e., six predefined ISIs were possible). Each possible ISI value occurred once in a run. The vicarious pain consisted of a video of a syringe held by a human adult male hand approaching-and-pricking with the needle the virtual hand in the muscle located between the index finger and the thumb. The vicarious pain involved only the virtual hand (observation only). Participants were not exposed to any somatosensory stimuli in this period. The vicarious pain video was pre-recorded and simulated with a fake syringe and needle (i.e., the needle was retractable). Two videos were recorded: one with a virtual male hand and one with a virtual female hand, both cropped so that the onset of the needlestick prick occurred at the same time (~3 s after the video onset). The vicarious pain videos were gender-matched to participants. The same video was presented on all blocks. No visibility manipulations were applied to these videos.

2.2.5. Subjective ratings

After the VHI, vicarious pain, and baseline fMRI (third element of the block - fixation cross for 8.96 s) periods, the fourth element was the rating of VHI statements, which lasted 18 s. Three statements were presented: (1) the Embodiment-1 statement – "*It seemed like the touch I felt was caused by the brush touching the virtual hand"; (*2) the Embodiment-2 – "*It seemed like the virtual hand belonged to me*"; (3) the Control statement – "*I found the experience enjoyable*". Based on their compatibility with our experimental setup, the three VHI statements corresponded to items 8, 3, and 20 described in (Longo et al., 2008b), respectively. While Embodiment-1 and Embodiment-2 are expected to assess different degrees of embodiment-related perceptions, the Control statement does not address embodiment-related aspects of illusory ownership. We selected these statements based on their (i) compatibility with our experimental setup, and (ii) ability to specifically measure only embodiment or other aspects of the VHI without being sensitive to other aspects. Under this light, we screened a referent psychometric classification of rubber hand statements (Longo et al., 2008b). First, we looked

for a statement with high embodiment values, and high communalities values, both in synchronous and asynchronous stimulation, resulting in the selection of Longo's item #3 as our Embodiment-1 statement. Second, we looked for a statement still related to embodiment, but to a lesser extent compared to the first one. Based on its low values in embodiment and communalities, we selected Longo's item #8 as our Embodiment-2 statement. Finally, we looked for a statement without links to embodiment nor to relatively closer aspects like "loss of own hand" or "movement". On this basis, we selected a statement related to "affect" and with the highest values for both affect and communalities (statement #20 from Longo et al. 2008b). This corresponded to our Control statement.

Participants rated their agreement with the three VHI statements by moving a continuous slider on a horizontal visual analogic scale, by means of two buttons on the response pad (by shortly pressing or holding them) with the index and middle fingers of the right hand. The VHI statements were always presented in the same order, with white text on a black screen, and participants had 6 s to complete each rating, which was indicated by an arc that moved clockwise and gradually changed from green to red until it completed a full circle. Participants were instructed that the far left and far right responses corresponded to "strongly disagree" and "strongly agree" with the statements, respectively. At the end of 6 s, the on-screen rating was recorded as the final answer given by the participants. Participants were also trained beforehand using a laptop to provide their ratings in a timely manner.

2.3. Data acquisition

2.3.1. MRI and psychometric data acquisition

We acquired functional and anatomical MR images using a Philips Achieva 3T MRI scanner upgraded to the dStream platform and a 32-channel head coil (Philips Healthcare, Best, The Netherlands). fMRI data were acquired using a T2*-weighted gradient-echo planar imaging sequence with repetition time = 2000 ms, echo time = 30 ms, flip angle = 80°, field-of-view = 240 × 240 mm^2, and voxel size = 3 × 3 × 4 mm^3. 37 axial slices were aligned parallel to the commissural line with an interslice gap of 0.5 mm and were acquired in ascending order to cover the entire cerebrum (the cerebellum was not completely covered in some participants). A total of 350 functional volumes were acquired per run (acquisition was longer than stimulus presentation to ensure recording of all experimental data) with a duration of 11 min40 s. 5 dummy scans were performed prior to each functional acquisition to establish steady-state magnetization. High-resolution anatomical MR images were acquired using a T1-weighted 3D magnetization-prepared gradient echo (MPRAGE) sequence with repetition time = 7.2 ms, echo time = 3.4 ms, flip angle = 8°, field-of-view = 240 × 240 mm^2, and isotropic voxel size = 1 mm^3. A total of 170 slices were acquired over 3.5 min. All image files were saved and analyzed in NIfTI (Neuroimaging Informatics Technology Initiative) format.

Stimulus onset and duration, participants' indication of perceived illusion, time to illusion onset, ratings of VHI statements for each combination of conditions and for each run and participant were stored in .mat files. Data collection began with the acquisition of a high-resolution anatomical image, followed by an initial on-screen message reminding participants of the experimental task. Next, a 1 s on-screen message reading "Experiment starting" was shown after the dummy scans, followed by the experimental protocol (Fig. 1). Due to technical issues, fMRI data from only three (instead of four) runs from five participants were acquired. Also due to technical issues, one participant's run contained fewer volumes (322 instead of 350), but because the acquisition was interrupted during the last rating of VHI statements, this run was included in the analysis.

2.3.2. Skin conductance measurement

In addition to subjective measurements of illusory hand ownership (VHI statements), we also designed the experiment to include an objective measurement of VHI. In typical RHI experiments the so-called proprioceptive drift is used as such an objective measure. However, in setups based on video recordings determining the actual distance between the real and virtual hand is much more difficult (Riemer et al., 2019). Therefore, we included estimates of threat-evoked SCR as an objective measure of VHI. Acknowledging that SCR can be measured even during the visuo-tactile stimulation period (Braithwaite et al., 2014; D'Alonzo et al., 2020), we nevertheless chose to evaluate SCR in response to a threat for two key reasons. First, using a threat is in line with previous evidence that skin conductance increases in response to threatening an embodied dummy hand (Armel and Ramachandran, 2003; Guterstam et al., 2013; Reinersmann et al., 2013). This approach assumes that the threat would amplify the physiological response, which would facilitate linking heightened SCR with illusory ownership. Second, the threat provides a clear and precise onset, which is crucial for conducting a General Linear Model (GLM) analysis to estimate the beta values of SCR. Without such an onset, accurately identifying and analyzing the response, such as during the visuo-tactile stimulation, would be more challenging. Therefore, the use of a threat enhances both the robustness of the physiological measure and the precision of our analysis.

During the vicarious pain period, in addition to brain activity, skin conductance was measured with a galvanic skin response device (PowerLab 4/35 and Bridge Amp, ADInstruments, UK). The galvanic skin response device, the amplifier, and a dedicated laptop equipped with the ADInstruments LabChart software were installed in the MR control room. The electrode cables were positioned parallel to the direction of the scanner bore, passed through the waveguide of the MR room, arrived to the control room, and were connected to the amplifier. The robot-controlling desktop computer triggered the onset of the galvanic skin response device acquisition to the visuo-tactile stimulation. The duration of the skin conductance signal acquisition was set to last until the end of the fMRI acquisition. Data from each participant and run were stored in ADICHT format and later converted to .mat format using adinstruments_sdk_matlab (https://github.com/JimHokanson/adinstruments_sdk_matlab). Due to technical issues, data from one run of nine participants, two runs of one participant, and all runs of one participant were not recorded and therefore could not be analyzed.

2.4. Data analysis

2.4.1. Sample size

Prior to acquiring the experimental data, we determined the sample size based on a power analysis of pilot data. Using the same procedures described in Sections 2.4.6 and 2.4.7, the average contrast estimates across runs during vicarious pain from five participants (four runs for four subjects and two runs for one subject) were extracted from the region of interest (ROI) representing the left premotor cortex. We used the left premotor cortex as a representative region based on previous literature (Ehrsson et al., 2004; Pamplona et al., 2022c). Specifically, we extracted contrast estimates from vicarious pain trials following visuo-tactile stimulation for all unique combinations of Stimulation and Visibility levels. Using RStudio (PBC, Boston, MA, USA; https://rstudio.com/) and the 'esvis' library, we calculated Cohen's d for three representative comparisons: sync|high and async|high (0.066), sync|high and sync|mid (0.764), and sync|high and sync|low (0.495). Using the 'pwr' library, we applied the 'pwr.t.test' function with a significance level of 0.017 (i.e., 0.05 corrected with the Bonferroni method for three comparisons), power of 80 %, and a paired *t*-test, we obtained sample sizes > 2000, 21, and 45, respectively. We chose the sample size of 45 for the study, which would be sufficient to evaluate differences in visibility for synchronous visuo-tactile stimulation.

2.4.2. Subjective ratings

We evaluated whether the subjective indication of perceived illusion and illusion-related subjective ratings (i.e., time to illusion onset and

VHI statements) were modulated by experimental conditions. First, for each subject, run, and combination of condition levels, the rating of VHI statements was converted to numbers using MATLAB and stored as a .csv file. These ratings were proportional to the final position of the slider on the horizontal scale, where the far left, center, and far right positions corresponded to 0, 50, and 100, respectively. The presence and absence of perceived illusion were represented by ones and zero, respectively. The time to illusion onset corresponded to the indication of perceived illusion minus the visuo-tactile stimulation onset. Only times to illusion onset from trials in which a perceived illusion was indicated were considered for analysis. Times to illusion onset lower than 4 s were discarded because they were shorter than the time of the first sinusoidal robotic movement, potentially indicating a misunderstanding of the instructions. We also discarded the following data: rating of Embodiment-1 statement from one participant in the first block due to self-reported insufficient time to rate the statement; indication and time to illusion onset from one participant in all runs, one participant in the first two runs, and one participant in the first run due to misinterpretation of the instruction to indicate the perceived illusion during the experiment; indication and time to illusion onset from one participant in the first run due to technical issues with data recording; all subjective measurements from two participants in one run due to technical failure of the robot; rating of Embodiment-1 and Embodiment-2 statements from one participant in the first two blocks due to self-reported inaccurate responses; indication and time to illusion onset from one participant in the first run due to self-reported negligence in indicating the perceived illusion; and all subjective measurements from one participant in two runs due to misinterpretation of the instructions.

Using RStudio, we investigated the dependence of subjective measurements on experimental conditions. We used linear mixed-effects models ('lmer' function, 'lmerTest' package) for the rating of VHI statements and the times to illusion onset and generalized linear mixed-effects models ('glmer' function, 'lme4' package) for the proportion of perceived illusions. We specified Visibility, Stimulation, and Run as fixed effects, and the participants as random effects. The 'anova' function was used to test the significance of the main effects and the interactions of the fixed effects. We calculated the coefficient of determination for significant main effects and interactions as a measure of their effect size of the model using the 'r2beta' function in the 'r2glmm' package and the Kenward-Roger approach. Post-hoc analyses of significant main effects and interactions were performed to determine significant pairwise differences at $p < 0.05$, Šidák-corrected for multiple comparisons. Post-hoc analyses were performed with the 'emmeans_test' function within the 'rstatix' package for the ratings of VHI statements and with the 'lsmeans' function within the 'lsmeans' package for the proportion of perceived illusions. The Cohen's d effect size of significant pairwise differences was calculated using the 'coh_d' function within the 'esvis' package for the ratings of VHI statements and the 'eff_size' function within the 'emmeans' package for the proportion of perceived illusions. The RStudio functions and packages used for linear mixed effects, Analysis of Variance (ANOVA), coefficient of determination, post-hoc analysis, and Cohen's d effect size for the following described analyses were the same as those used for the ratings of VHI statement, except where noted.

2.4.3. Objective measure

We investigated the dependence of skin conductance response estimates on experimental conditions, reflecting modulation of unconscious illusory hand ownership. For each subject and run, the skin conductance time-series was first filtered using MATLAB to remove MRI-related artifacts and other nuisance sources from the signal via the following steps. First, we computed the discrete Fourier transform of the time-series for each subject and run, to obtain the power spectrum over the frequency components. Then, we identified and removed the frequency components with extreme outlier magnitude, mainly indicating the interference of MRI gradients in the galvanic skin response recording. Time-series cleaning was performed by checking whether the maximum magnitude of frequency components between 0.03 and 0.7 Hz (with a temporal resolution of 0.001 Hz) was greater than a threshold defined by the mean plus ten standard deviations of the power values within this range. If the maximum magnitude of a given frequency component was greater than the threshold, that frequency component was removed from the power spectrum using a notch filter with a width of 0.0001 Hz. This process of removing frequency components with extreme outlier magnitude was computed iteratively until all outliers were removed. The power spectrum without extreme outlier frequency components was then converted back into a time-series using the inverse Fourier transform, resulting in a filtered skin conductance time-series. We also applied a passband filter with cut-off frequencies of 0.005 and 5 Hz to remove low and high frequency components.

We then estimated the betas of the skin conductance response estimates for each run and participant using the GLM approach with the PsPM toolbox (Bach and Friston, 2013). We constructed regressors with boxcar functions corresponding to each unique combination of condition levels, specifying the onset of the vicarious pain videos (i.e., immediately after the interstimulus interval) and a duration of ten seconds. These boxcar functions were convolved with a canonical skin conductance function as provided by the PsPM toolbox. Finally, we used linear mixed-effects models with RStudio defining the skin conductance response estimates as the dependent variable, the factors Visibility (high, medium, low), Stimulation (sync, async), and Illusion (yes, no) as fixed effects, and the participant as random effects. The factor Visibility refers to the degree to which the virtual hand was visible to participants, with three levels: high (clear view), mid (weak "crystallization"), low (strong "crystallization"). The factor Stimulation represents the coherence between the visual strokes of the virtual hand and the tactile stroking of the participant's hand, including two levels: synchronous (the visual and the tactile stroking follow the same spatio-temporal profile), asynchronous (different spatio-temporal profiles of the visual and tactile stroking). The Illusion factor indicates whether the participant reported the perceived illusion during the visuo-tactile stimulation. We tested the significance of the main effects and the interactions of the fixed effects. We computed the coefficient of determination for significant main effects and interactions as a measure of their effect size. We performed post-hoc analyses of significant main effects and interactions to determine significant pairwise differences at $p < 0.05$, Šidák-corrected for multiple comparisons, and calculated their Cohen's d effect sizes.

2.4.4. MRI preprocessing

Prior to statistical analyses, fMRI data acquired during the experiment from all participants and runs were preprocessed using SPM12 (Statistical Parametric Mapping – www.fil.ion.ucl.ac.uk) in MATLAB. First, the fMRI data were slice-time corrected using the middle slice as a reference. Next, six rigid-body parameters of head motion (translation and rotation) were estimated from the resulting functional images, which were then spatially realigned, and a mean functional image was generated. Next, the anatomical image was coregistered to the mean functional image and used to create a deformation field for the spatial normalization of the fMRI to the Montreal Neurological Institute (MNI) stereotactic space with voxel size $2 \times 2 \times 2$ mm^3. Finally, the resulting functional images were spatially smoothed with a Gaussian kernel of 6-mm^3 full-width at half maximum. Prior to statistical analysis, fMRI runs were cropped to 330 vol. We used the Artifact Detection Tools (ART) toolbox (www.nitrc.org/projects/artifact_detect/) to flag volumes with excessive head motion. One participant showed excessive head motion (> 4 mm) in all acquisitions and was removed from fMRI analysis.

2.4.5. Estimation of subject-specific brain activation: Model1/VHI

We investigated how brain activation varied across conditions during visuo-tactile stimulation (Model1/VHI) computing individual GLMs using SPM12. We defined three factors for this analysis: Visibility,

Stimulation, and Time. The factors Visibility and Stimulation are described in 2.4.3. The factor Time had two levels, "Early" and "Late", modeled as the first and second halves of the visuo-tactile stimulation (duration 32.1 s), respectively. We constructed the design matrix with twelve regressors of interest to represent each unique combination of condition levels (2 Stimulation x 3 Visibility x 2 Time levels) using boxcar functions specifying the onset and duration of the visuo-tactile stimulation for each run and participant. We also included regressors of no-interest to the design matrix to represent the periods of vicarious pain, baseline, and subjective rating of VHI statements. For trials in which the illusion was indicated, we also included a regressor of no-interest representing button presses as stick functions (i.e., with zero duration). The design matrix was complete with regressors of no-interest representing the six estimated parameters of head motion and binary regressors representing volumes flagged with excessive movement. The regressors were then convolved with a canonical hemodynamic response function (HRF). Then, for each run and participant, we estimated the GLM beta weights for each regressor simultaneously. We used a high-pass filter with a cut-off of half the run duration (Nurmi et al., 2018) and a first-degree auto-regressive model to remove low-frequency fluctuations and temporal autocorrelation in the time-series. We then computed participant-specific maps for simple contrast and for a three-way repeated-measures ANOVA with the main effects of Visibility, Stimulation, and Time, as well as their interaction, on the activation. The procedure was based on (Henson, 2015), which partitions the error and reduces the chance of false positives. Finally, average contrast maps across runs were calculated for each participant.

2.4.6. Estimation of subject-specific brain activation: Model2/Vicariousness

We also investigated how activation varied across conditions during vicarious pain (Model2/Vicariousness) using individual GLMs. Only the factors Visibility and Stimulation were used for this analysis, which are related to the stimulation received during the visuo-tactile stimulation. We constructed the design matrix with six regressors of interest (2 Stimulation x 3 Visibility levels). We constructed the regressors with boxcar functions specifying the onset of vicarious pain and a duration of 5 s (i.e., only the first half of the period). For this model, we assumed that the time-to-peak response to vicarious pain across participants would have a high variance (Pamplona et al., 2022c). Thus, in addition to regressors convolved with the canonical HRF, we also incorporated the first derivative of the HRF to capture the variance in time-to-peak. Regressors of no-interest representing visuo-tactile stimulation, baseline, and rating of VHI statements, as well as the six estimated parameters of head motion and the binary regressors representing volumes with excessive movement were convolved with the canonical HRF and included in the design matrix. Next, for each run and participant, we estimated the beta simultaneously. The high-pass filter and the first-degree auto-regressive model were applied, as described in the previous section. We then calculated simple contrast and ANOVA maps as described in the previous section and averaged them across runs. Finally, a "boosted" contrast map was obtained for each combination of condition levels and subject as a function of the canonical and derivative terms of the model according to previous work (Calhoun et al., 2004).

2.4.7. ROI definition and analysis

We investigated the dependence of activation on conditions during visuo-tactile stimulation and vicarious pain in predefined ROIs. A total of 21 six-mm-radius spherical ROIs were built using the MarsBaR toolbox (marsbar.sourceforge.net/; Brett et al., 2002) (Table 1). The centers of 17 of these ROIs were meta-analytic peaks (http://www.neurosynth.org; Yarkoni et al., 2011) of regions commonly associated with illusory hand ownership (Bekrater-Bodmann et al., 2014; Ehrsson et al., 2005; 2004; 2007b; Ionta et al., 2011; Limanowski et al., 2014b; Naito et al., 2002; Nilsson and Kalckert, 2021; Pamplona et al., 2022c; Tsakiris, 2010) and from a previous study on tactile- and vision-related neural responses of body ownership (Pamplona et al., 2022c). These ROIs represented the supplementary motor area (SMA), bilateral anterior insula (INS), premotor cortex (PMC), primary motor cortex (M1), supramarginal gyrus (SMG), intraparietal sulcus (IPS), fusiform body area (FBA), lingual gyrus (LING), and primary visual cortex (V1). The other four ROIs were centered on coordinates from a study on the somatotopic organization of the hand in the brain, converted to the MNI space using the function 'tal2icbm_spm' (www.brainmap.org/icbm2tal/). These four ROIs represented the primary (S1) and secondary (S2) somatosensory cortex. Detailed information about all ROIs is reported in Table 1.

For Models 1/VHI and 2/Vicariousness, we averaged the beta values within each ROI for each combination of condition levels, run, and subject. Beta values corresponded to estimates based on the canonical HRF and to the estimates based on the canonical HRF and its first derivative for Model1/VHI and Model2/Vicariousness, respectively. Binary values, representing the presence or absence of perceived illusion during the visuo-tactile stimulation were assigned to each beta value. Using RStudio, we calculated linear mixed-effects models to evaluate the condition-specific dependence of ROI-specific betas, and tested the

Table 1
ROI specifications.

Brain Area	Source	Hemisphere	#	Acronym	MNI coordinates (x, y, z)
Intraparietal sulcus	Meta-analysis (intraparietal sulcus)	Left	1	L-IPS	−30, −50, 42
		Right	2	R-IPS	40, −38, 44
Premotor cortex	Meta-analysis (premotor)	Left	3	L-PMC	−30, −12, 60
		Right	4	R-PMC	26, −8, 56
Primary visual cortex	Meta-analysis (inferior occipital)	Left	5	L-V1	−34, −88, −10
		Right	6	R-V1	36, −86, −12
Primary motor cortex	Meta-analysis (primary motor)	Left	7	L-M1	−38, −18, 56
		Right	8	R-M1	38, −20, 62
Supplementary motor area	Meta-analysis (supplementary motor)	Medial	9	SMA	−2, −8, 66
Anterior insular cortex	Meta-analysis (anterior insula)	Left	10	L-INS	−35, 18, −1
		Right	11	R-INS	38, 18, 0
Fusiform body area	Meta-analysis (fusiform gyrus)	Left	12	L-FBA	−38, −48, −18
		Right	13	R-FBA	40, −46, −18
Lingual gyrus	Meta-analysis (lingual)	Left	14	L-LING	−14, −70, −4
		Right	15	R-LING	18, −70, −6
Supramarginal gyrus	Meta-analysis (supramarginal gyrus)	Left	16	L-SMG	−62, −26, 32
		Right	17	R-SMG	58, −32, 40
Primary somatosensory cortex	Extracted from Bingel et al.	Left	18	L-S1	−38, −37, 57
		Right	19	R-S1	39, −37, 58
Secondary somatosensory cortex	Extracted from Bingel et al.	Left	20	L-S2	−45, −16, 14
		Right	21	R-S2	49, −17, 16

significance of main effects and interactions of the fixed effects. For Model1/VHI, we defined four fixed effects: Visibility, Stimulation, Time, and Illusion. For Model2/Vicariousness, we defined three fixed effects: Visibility, Stimulation, and Illusion. Participants were defined as random effects. The significance level was set at 0.05, corrected for multiple comparisons across ROIs using the Benjamini-Hochberg false discovery rate (FDR) method for each model. We calculated the coefficient of determination for significant main effects and interactions as a measure of their effect size. We performed post-hoc analyses to determine significant pairwise differences, Šidák-corrected for multiple

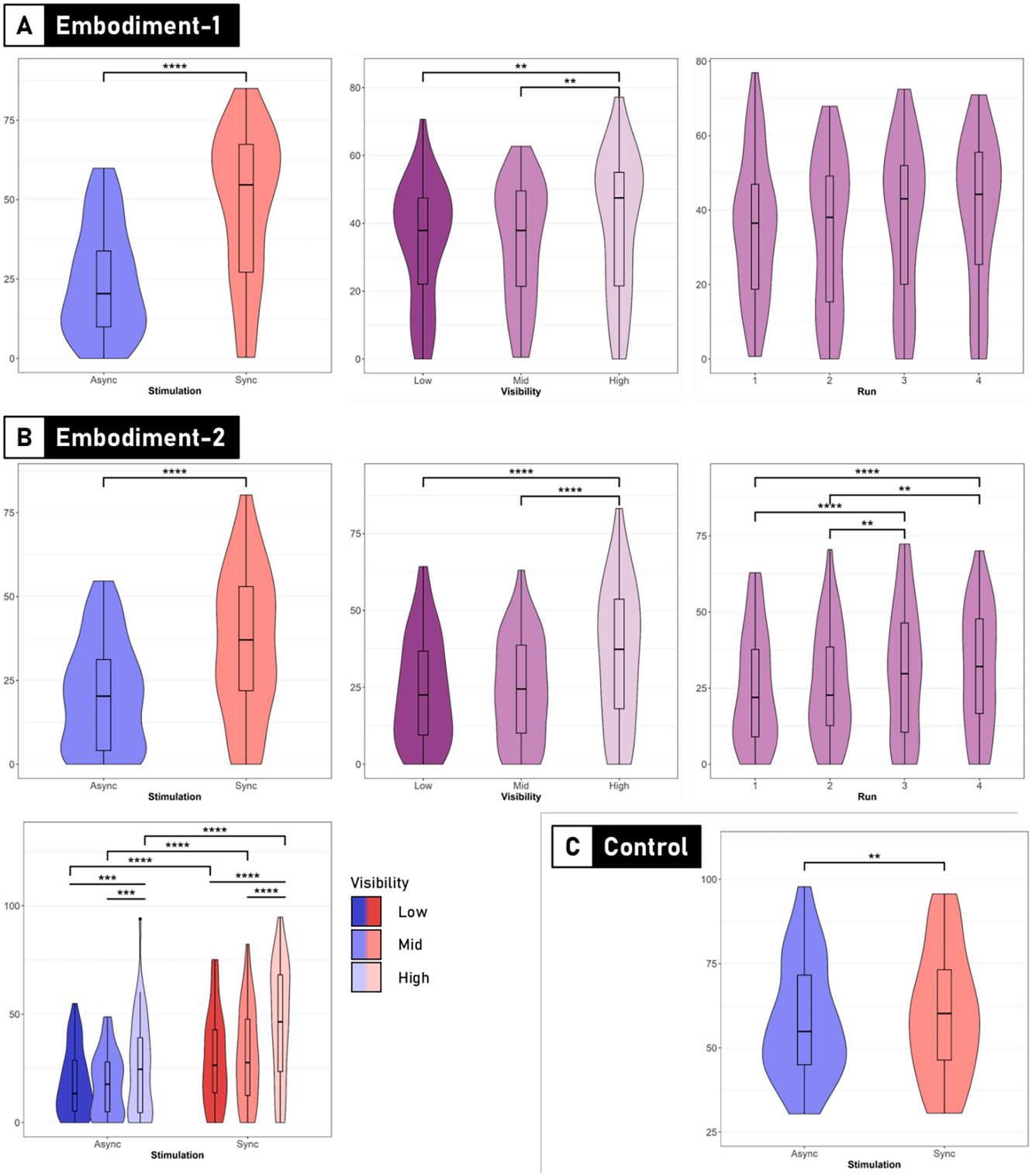

Fig. 2. Subjective rating. Significant main effects and interactions on ratings of Embodiment-1 (A), Embodiment-2 (B), and Control (C) statements following linear mixed-effects models (with three factors: Stimulation, Visibility, and Run). Results for synchronous and asynchronous visuo-tactile stimulation are shown in red and blue, respectively. Results where synchronous and asynchronous visuo-tactile stimulation are grouped together are shown in purple. Dark, medium, and light colors represent low, medium, and high visibility, respectively. Asterisks represent significant differences in post-hoc analyses corrected for multiple comparisons using Šidák's correction (****$p < 0.0001$, ***$p < 0.001$, **$p < 0.01$). Sync = synchronous, Async = asynchronous, Mid=medium.

comparisons, and calculated their Cohen's d effect sizes.

2.4.8. Group-level whole-brain analyses

We also investigated mapped the whole brain for the dependence of activation clusters on the conditions for visuo-tactile stimulation and vicarious pain. Using SPM12, we computed group-level whole-brain repeated-measures ANOVA for both Models for the factors previously defined in the first-level analysis. For each main effect and interaction, participant-specific ANOVA contrasts, computed as described in Sections 2.4.5 and 2.4.6, were included in a one-way ANOVA test to compute F/t-values (which is the recommended procedure for whole-brain repeated-measures ANOVA in SPM; Henson, 2015). The Illusion factor, included in the ROI analysis, could not be used in the whole-brain repeated-measures ANOVA because of its trial dependency, which would lead to unbalanced design. We used a cluster-threshold p-value of 0.05, family-wise error (FWE) corrected for multiple comparisons for the main effects of Model1/VHI. For illustrative purposes only, due to the low effect size of the results for interactions in Model1/VHI and main effects and interactions of Model2/Vicariousness [see Effect size (partial η^2) in Tables S3 and S6], we used rather liberal cluster-threshold p-values (uncorrected 0.001 for 2-way interactions in Model1/VHI and main effects and interactions in Model2/Vicariousness; uncorrected 0.005 for the 3-way interaction in Model1/VHI). Resulting clusters were labeled by the Anatomy Toolbox, implemented in the bspmview toolbox (www.bobspunt.com/bspmview), and by XjView (www.alivelearn.net/xjview). We averaged contrast values within significant clusters to compute the partial η^2 as a measure of effect size of the main effects and interactions, and to perform post-hoc analyses to investigate pairwise differences.

2.4.9. Associations of brain activity with subjective VHI ratings and physiological measures

We further investigated whether activation in predefined ROIs was associated with rating of VHI statements (subjective measure) or skin conductance response to vicarious pain (objective measure) for Model1/VHI and Model2/Vicariousness. We used trial-specific betas computed for each ROI as dependent variables. For each Model and ROI, we computed linear mixed-effects models and tested the significance of main effects and interactions for fixed effects. For this analysis, we defined two fixed effects: Rating (for subjective measures) and skin conductance response (for objective measures) and Illusion. Participants were defined as random effects. The significance level was set to 0.05, with each main effect and interaction corrected for multiple comparisons across ROIs using FDR for each model. We computed the coefficient of determination for significant main effects and interactions as a measure of their effect size. We report regression parameters and statistics of all significant associations.

3. Results

3.1. Subjective ratings

For Embodiment-1 statement our analysis revealed a significant main effect of Stimulation on rating [$F(1955) = 377.22$, $p < 0.0001$], with higher ratings for synchronous ($M = 48.4$, $SD = 23.6$) compared to asynchronous visuo-tactile stimulation ($M = 24.2$, $SD = 17.1$) (Fig. 2A). We also observed a significant main effect of Visibility on rating ($F(2955) = 8.22$, $p = 0.0003$), with higher ratings for high ($M = 39.9$, $SD = 20.5$) compared to medium ($M = 34.3$, $SD = 17.7$) and low visibility ($M = 34.6$, $SD = 17.7$) (Fig. 2A). We also observed a significant main effect of Run on the rating [$F(3957) = 3.45$, $p = 0.016$)], with higher ratings associated with later runs (run1: $M = 35.4$, $SD = 18.8$; run2: $M = 34.2$, $SD = 20.3$; run3: $M = 37.4$, $SD = 20.9$; run4: $M = 38.9$, $SD = 20.4$), but no significant pairwise differences (Fig. 2A). Effect-sizes, t-values, and p-values of significant pairwise differences in the post-hoc analysis for the Embodiment-1 statement are reported in Table S1.

For Embodiment-2 statement our analysis revealed a significant main effect of Stimulation on rating [$F(1956) = 173.64$, $p < 0.0001$], with higher ratings for synchronous ($M = 35.4$, $SD = 21.5$) compared to asynchronous visuo-tactile stimulation ($M = 20.4$, $SD = 16.0$) (Fig. 2B). We also observed a significant main effect of Visibility on rating [$F(2956) = 48.64$, $p < 0.0001$], with higher ratings for high ($M = 35.4$, $SD = 22.3$) compared to medium ($M = 24.5$, $SD = 16.8$) and low visibility ($M = 23.8$, $SD = 17.3$) (Fig. 2B). We also observed a significant main effect of Run on rating [$F(3958) = 12.44$, $p < 0.0001$], with higher ratings for the third ($M = 30.5$, $SD = 21.4$) and fourth ($M = 31.3$, $SD = 20.0$) compared to the first ($M = 24.4$, $SD = 18.6$) and second runs ($M = 26.3$, $SD = 18.2$) (Fig. 2B). We also observed the significant interaction between Stimulation and Visibility on rating [$F(2956) = 7.26$, $p = 0.0007$], showing (1) higher ratings for high visibility compared to medium and low visibility, both after synchronous (high: $M = 46.0$, $SD = 26.8$; medium: $M = 31.2$, $SD = 21.8$; low: $M = 29.2$, $SD = 21.4$) and asynchronous visuo-tactile stimulation (high: $M = 24.9043$, $SD = 22.0$; medium: $M = 17.8$, $SD = 14.5$; low $M = 18.4$, $SD = 15.3$), and (2) higher ratings for synchronous compared to asynchronous visuo-tactile stimulation, matched for visibility (Fig. 2B). Effect-sizes, t-values, and p-values of significant pairwise differences in the post-hoc analysis for Embodiment-2 statement are reported in Table S1.

For the Control statement, we found only a significant main effect of Stimulation on rating [$F(1958) = 7.92$, $p = 0.005$], with higher ratings for synchronous ($M = 60.0$, $SD = 18.7$) compared to asynchronous visuo-tactile stimulation ($M = 58.1$, $SD = 17.5$) (Fig. 2C). Effect-sizes, t-values, and p-values of significant pairwise differences in the post-hoc analysis for the Control statement are reported in Table S1. Ratings of Embodiment-1 and Embodiment-2 statements were correlated with each other ($r = 0.7$, adj. $p < 0.0001$), but not with the Control statement ($r = 0.06$, adj. $p = 0.07$; $r = -0.06$, adj. $p = 0.06$, respectively).

3.2. Illusion perception

The proportion of participants who reported perceiving the illusion in at least one of the trials in 25 %, 50 %, 75 %, and 100 % of runs was 73.3 %, 48.9 %, 33.3 %, and 17.8 %, respectively. Using a three-factor chi-squared test (Stimulation, Visibility, and Run), we observed main effects of Stimulation [$X^2(1) = 57.21$, $p < 0.0001$)], Visibility [$X^2(2) = 31.51$, $p < 0.0001$], and Run [$X^2(3) = 14.17$, $p = 0.0027$] on the proportion of perceived illusions, but no significant two- or three-way interactions (Fig. 3A). Post-hoc analysis revealed that there was a higher proportion of perceived illusions for high compared to medium and low visibility, for synchronous compared to asynchronous visuo-tactile stimulation, and for the fourth compared to the first run. Effect sizes, z-values, and p-values from these significant pairwise differences in the post-hoc analyses are shown in Table S1. Using a linear mixed-effects model with three factors (Stimulation, Visibility, and Run), we observed no main effects or interactions of experimental conditions on the time to illusion onset (Fig. S1).

3.3. Skin conductance response to vicarious pain

Using linear mixed-effects models with three factors (Stimulation, Visibility, and Illusion), we observed a significant interaction Illusion x Stimulation on the estimate of skin conductance response to vicarious pain [$F(1929) = 5.38$, $p = 0.021$] (Fig. 3B, Table S1). Post-hoc analysis revealed no significant pairwise differences. The estimate of skin conductance response to vicarious pain tends to be larger for synchronous compared to asynchronous visuo-tactile stimulation when illusion is perceived ($p = 0.10$, $d = 0.22$). Conversely, when no illusion is perceived, the skin conductance related to vicarious pain tends to be larger after asynchronous compared to synchronous visuo-tactile stroking ($p = 0.054$, $d = -0.14$). The three-way and remaining two-way interactions and main effects were not statistically significant (all $p_s > 0.05$). The estimate of skin conductance response to vicarious pain

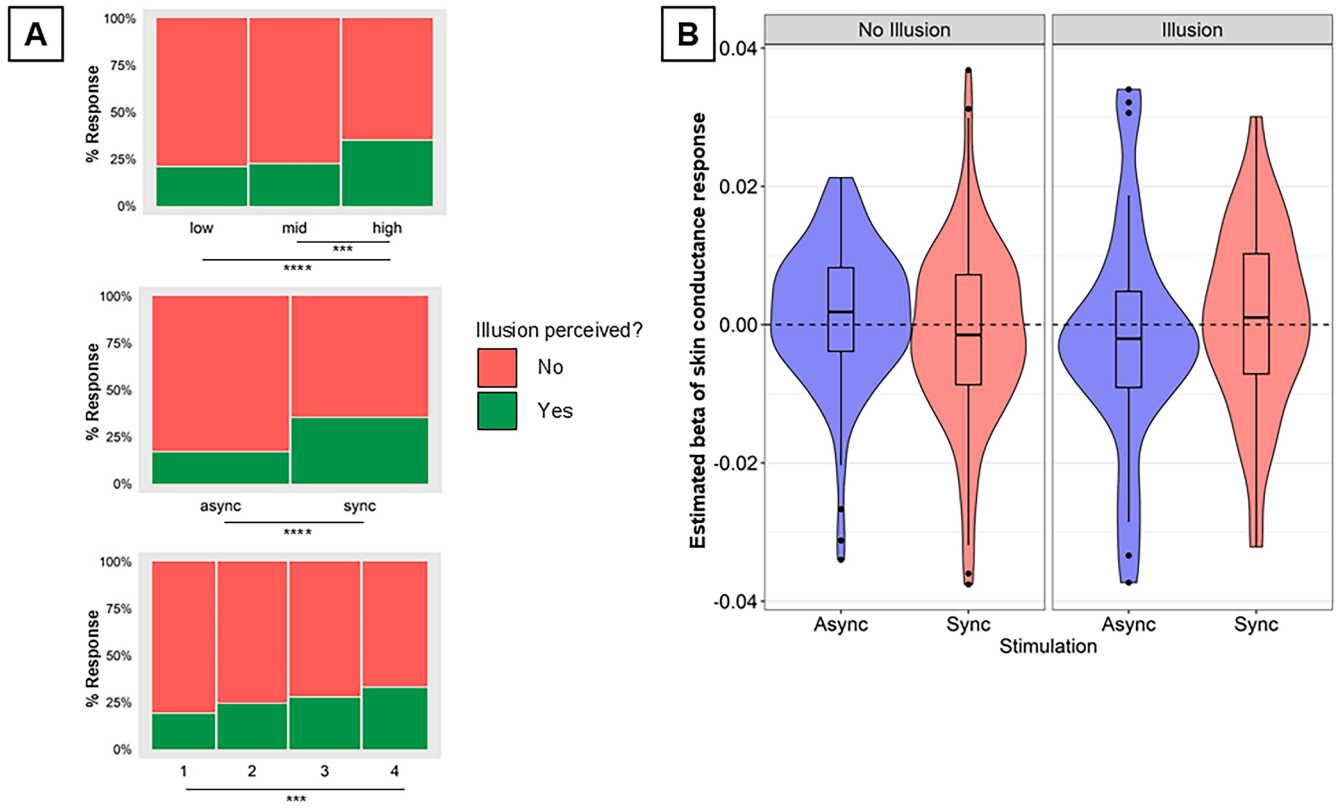

Fig. 3. The proportion of perceived illusions increases with synchronous (compared to asynchronous) visuo-tactile stimulation, with higher visibility, and over runs (A). The estimate of skin conductance response to vicarious pain tends to be higher for synchronous compared to asynchronous visuo-tactile stimulation when illusion is perceived, while the opposite is true when no illusion is perceived (B). In A, green and red colors represent trials with and without indication of perceived illusion, respectively. Asterisks represent significant differences in post-hoc analyses corrected for multiple comparisons using Šidák's correction (****$p < 0.0001$, ***$p < 0.001$). In B, Red and blue colors represent synchronous and asynchronous visuo-tactile stimulation, respectively. Sync = synchronous, Async = asynchronous, mid = medium.

was not associated with the ratings of VHI statements (all $p_s > 0.05$).

3.4. Estimation of brain activity

3.4.1. Model1/VHI

3.4.1.4. ROI analysis. Using linear mixed-effects models, we analyzed activation differences in all 21 ROIs during the VHI induction period with the factors Visibility, Stimulation, Time, and Illusion (Fig. 4; Table S2). In the right hemisphere, the main effect of Visibility was significant for the activation of R-V1 [$F(2,2035) = 6.55$, $p = 0.010$], R-FBA [$F(2,2036) = 5.79$, $p = 0.013$], R-IPS [$F(2,2037) = 6.86$, $p = 0.010$], and R-S1 [$F(2,2037) = 5.17$, $p = 0.019$], all showing higher activation for high compared to medium visibility (Fig. 5A; light blue in Fig. 4). In the left hemisphere, the main effect of Visibility was significant for L-V1 [$F(2,2037) = 5.06$, $p = 0.019$], L-FBA [$F(2,2037) = 8.04$, $p = 0.007$], and L-SMG [$F(2,2036) = 6.16$, $p = 0.011$], where the activity was higher during high compared to both medium and low visibility (Fig. 5A; light blue in Fig. 4). The main effect of Stimulation was significant only in the right hemisphere, namely for the activation of R-FBA [$F(1,2051) = 10.40$, $p = 0.027$] and R-S1 [$F(1,2052) = 8.57$, $p = 0.04$], with higher activation during synchronous compared to asynchronous visuo-tactile stimulation (Fig. 5B; red in Fig. 4). In the right hemisphere, the main effect of Time was significant for the activation of R-LING [$F(1,2032) = 16.95$, $p = 0.0005$], R-S1 [$F(1,2032) = 16.27$, $p = 0.0006$], and R-S2 [$F(1,2032) = 11.97$, $p = 0.0023$]. In the left hemisphere, the main effect of Time was significant for L-M1 ($F(1,2033) = 12.73$, $p = 0.0021$), L-LING ($F(1,2032) = 6.03$, $p = 0.049$), and L-SMG ($F(1,2036) = 12.53$, $p = 0.0021$). In L-M1, L-LING, and R-LING, the activity in the second half of visuo-tactile stimulation (Late) was higher than in the first half (Early; Fig. 5C; purple in Fig. 4). Conversely, in L-SMG, R-S1, and R-S2 the activity was lower in the second half of visuo-tactile stimulation than in the first half (Fig. 5C; blush pink in Fig. 4). Effect-sizes, t-values, and p-values of these significant pairwise differences in the post-hoc analysis are reported in Table S2. The interaction between Illusion and Stimulation was significant on the activation of SMA [$F(1,2059) = 10.41$, $p = 0.027$] (Fig. 5D; fuchsia in Fig. 4). The post-hoc analysis showed the significantly higher activation of SMA in trials where participants perceived the illusion for synchronous compared to asynchronous visuo-tactile stimulation. The post-hoc analysis also showed the higher activation in trials of synchronous visuo-tactile stimulation for perceived compared to non-perceived illusion. We found no ROIs with significant three- or four-way interactions.

3.4.1.5. Whole-brain analysis. The whole-brain analysis of the activity during the VHI-period was performed using a repeated-measures ANOVA with the factors Visibility, Stimulation, and Time (FWE-corrected voxel threshold of $p < 0.05$) (Table S3; Fig. 4). The main effect of Visibility was significant for the activation of the right extrastriate body area (R-EBA, coordinates: 48, −64, −2; cluster size = 179 voxels), left EBA (L-EBA; coordinates: −46, −74, −6; cluster size = 139 voxels), and R-V1 (coordinates: 14, −94, 14; cluster size = 26 voxels). Post-hoc analysis revealed that, with respect to medium and low visibility, the activation for high visibility was higher in L-EBA and R-EBA (Fig. 6A; light blue in Fig. 4) but lower in R-V1 (Fig. 6A; dark blue in Fig. 4). The main effect of Time was significant for the activation of several regions. In some clusters, the activation was higher in Late than Early phases of visuo-tactile stimulation, including a cluster comprising the posterior

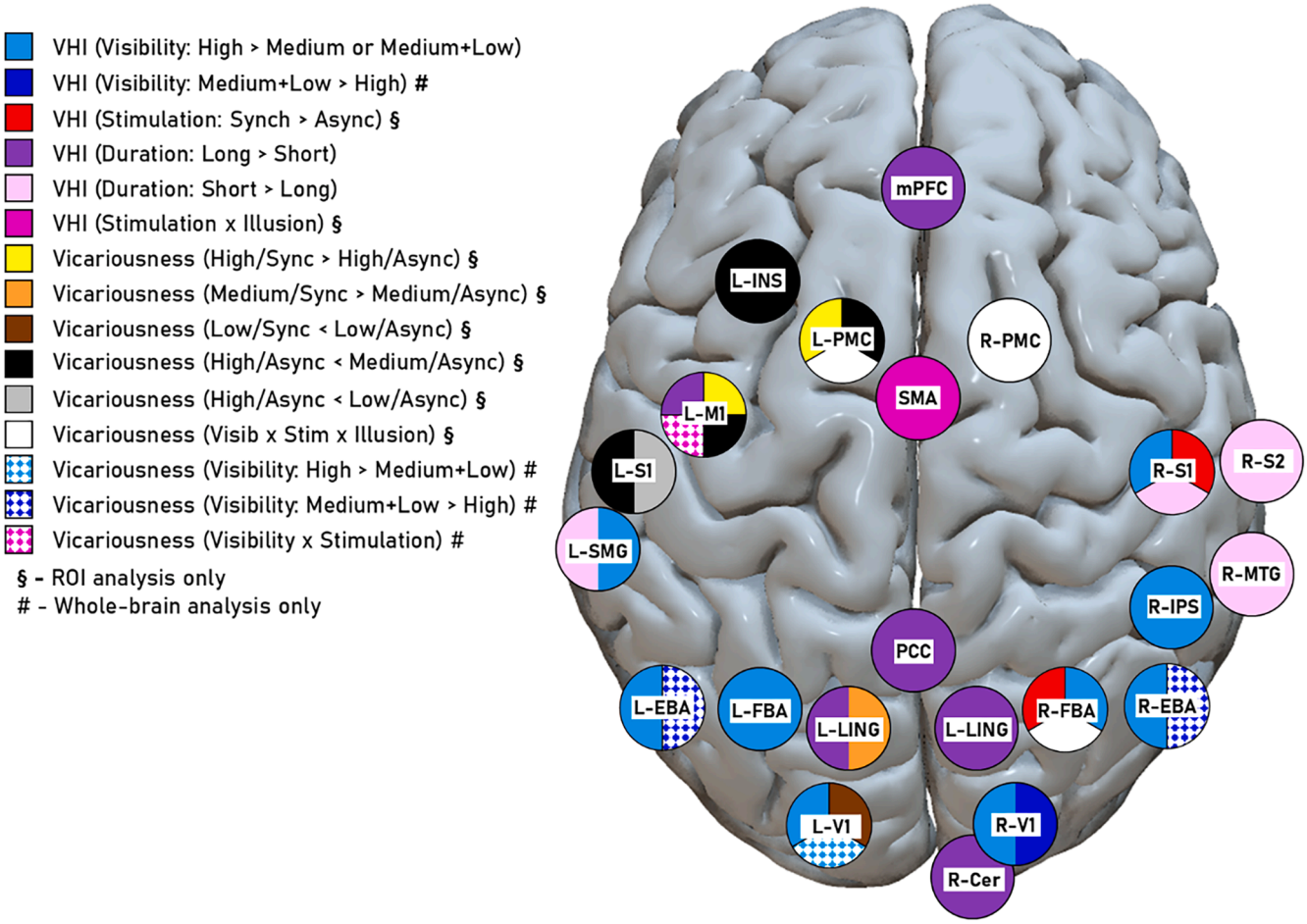

Fig. 4. Overview of brain activity. During visuo-tactile stimulation (VHI), (i) visibility manipulations influenced the activity of visual, somatosensory, and multisensory regions (light and dark blue), (ii) visuo-tactile synchrony modulated visual and somatosensory regions (red), and (iii) time of stimulation influenced visual, somatosensory, and multisensory regions (purple and blush pink). During the vicarious pain phase (Vicariousness), (i) visibility manipulations influenced the activity of visual regions (dotted light and dark blue), (ii) the interaction between visibility manipulations and visuo-tactile stimulations modulated the activity of visual, somatosensory, and motor regions (yellow, orange, brown, black, grey), and (iii) the interaction between Visibility, Stimulation, and Illusion was reflected by the activity of visual and motor regions (white). Abbreviations: L- (Left); R- (Right); m (medial); PFC (medial prefrontal cortex); INS (left insula); PMC (premotor cortex); SMA (supplementary motor area); M1 (primary motor cortex); S1 (primary somatosensory cortex); S2 (secondary somatosensory cortex); SMG (supramarginal gyrus); MTG (middle-temporal gyrus); IPS (inferior-parietal sulcus); PCC (posterior cingulate cortex); EBA (extrastriate body area), FBA (fusiform body area); LING (lingual gyrus); V1 (primary visual cortex); Cer (cerebellum).

cingulate cortex and cerebellum (PCC/CER; coordinates: 14, −60, −14; cluster size = 3055 voxels), medial prefrontal cortex (mPFC; coordinates: 12, 50, −6; cluster size = 2964 voxels), and L-M1 (coordinates: −38, −24, 70; cluster size = 186 voxels) (Fig. 6B; purple in Fig. 4). Conversely, activation decreased over time in another set of clusters, including R-S2 (coordinates: 56, −22, 22; cluster size = 116 voxels) and right middle temporal gyrus [R-MTG (coordinates: 48, −68, 8; cluster size = 77 voxels)] (Fig. 6B; blush pink in Fig. 4). Additional activation clusters showing the main effect of Time, as well as effect sizes, t-values, and p-values of significant pairwise differences in post-hoc analyses for the reported clusters are shown in Table S3. We found no significant activation clusters for the main effect of Stimulation.

Using a more liberal voxel threshold (unc. $p < 0.001$), our analysis revealed a significant two-way interaction Time x Stimulation on the activation of the L-SMG (coordinates: −62, −16, 18; cluster size = 22 voxels), corpus callosum (coordinates: 18, 12, 36; cluster size = 17 voxels), left inferior temporal gyrus (coordinates: −52, −2, −40; cluster size = 14 voxels), and right amygdala (coordinates: 28, −6, −12; cluster size = 14 voxels) during the visuo-tactile stimulation period (Fig. S2A). Our analysis also indicated a significant two-way interaction Time x Visibility on activation in the L-V1 (coordinates: −10, −94, 14; cluster size = 36 voxels) during the visuo-tactile stimulation period (Fig. S2B). No significant activation clusters were found for the interaction Stimulation x Visibility during the visuo-tactile stimulation period. Also using a liberal voxel threshold (unc. $p < 0.005$), we observed a significant three-way interaction (Time x Stimulation x Visibility) on the activation of the R-V1 (coordinates: 26, −90, 12; cluster size = 14 voxels) (Fig. S2C). The contrasts, effect-sizes, t-values, and p-values of significant pairwise differences in the post-hoc analysis for these clusters are reported in Table S3.

3.4.1.6. Brain-Perception correlations. The activation in the anterior insula during the late phase of visuo-tactile stimulation was associated with ratings of all three VHI statements (Fig. 7, Table S4). In particular, the activity of the right anterior insula (R-INS) was associated with ratings in the Embodiment-1 statement (main effect of Rating, slope = 0.0025 ± 0.0007, $R^2 = 0.24$, $p = 0.0008$) and the Embodiment-2 statement (main effect of Rating, slope = 0.0023 ± 0.0008, $R^2 = 0.23$, $p = 0.007$). We found a significant interaction between Illusion and ratings in the Control statement on activity in the L-INS ($R^2 = 0.26$; not perceived illusion: slope = 0.0003 ± 0.0024, $p = 0.9$; perceived illusion: slope = 0.012 ± 0.003, $p = 0.0019$). The estimated skin conductance

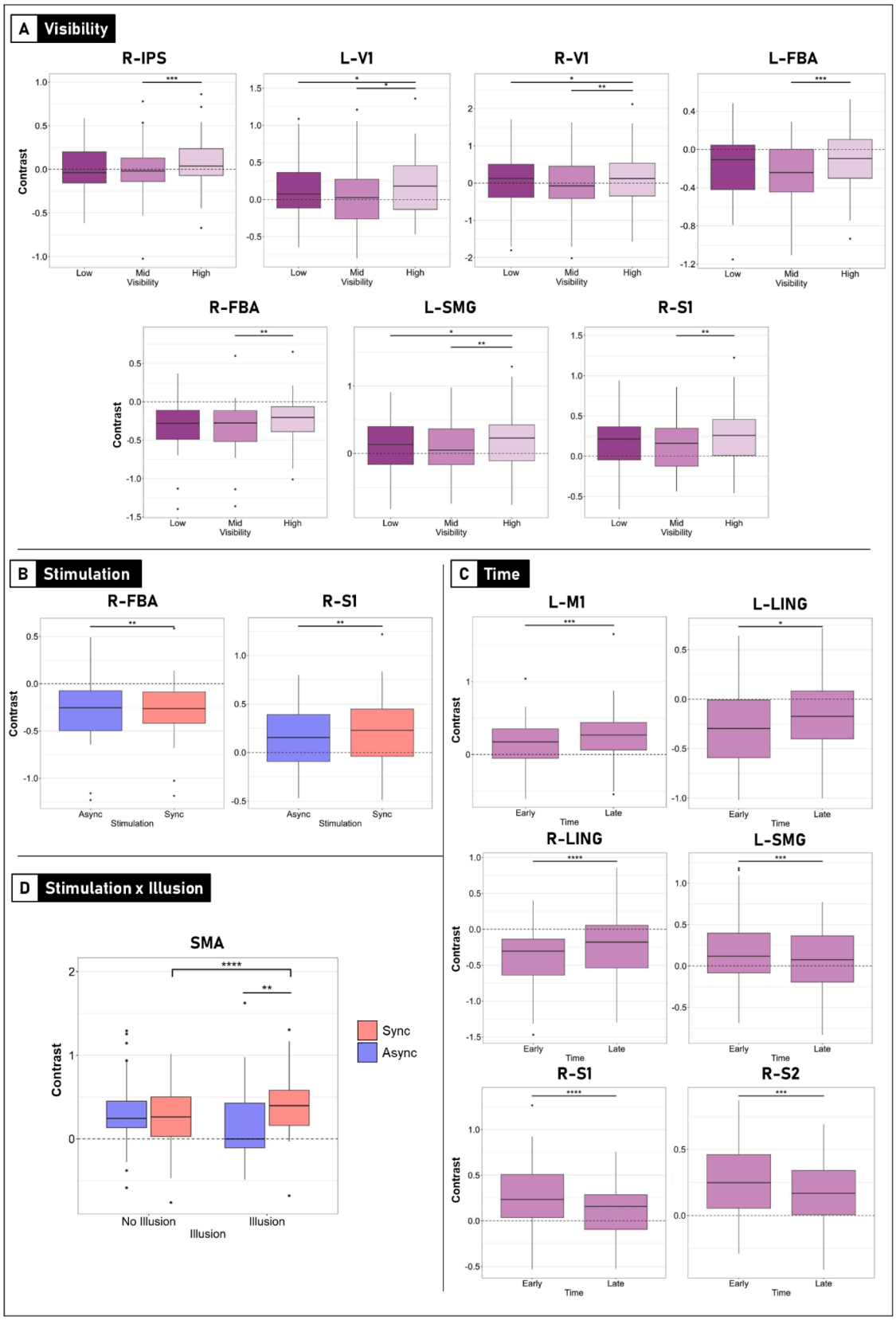

Fig. 5. ROI analysis of the VHI phase. Contrast differences in ROIs with significant interaction between Stimulation and Illusion, as well as significant main effects of Stimulation, Visibility, and Time on activation during visuo-tactile stimulation. Asterisks represent significant differences in post-hoc analysis corrected for multiple comparisons using Šidák's correction (****$p < 0.0001$, ***$p < 0.001$, **$p < 0.01$, *$p < 0.05$). Abbreviations correspond to those of Fig. 4.

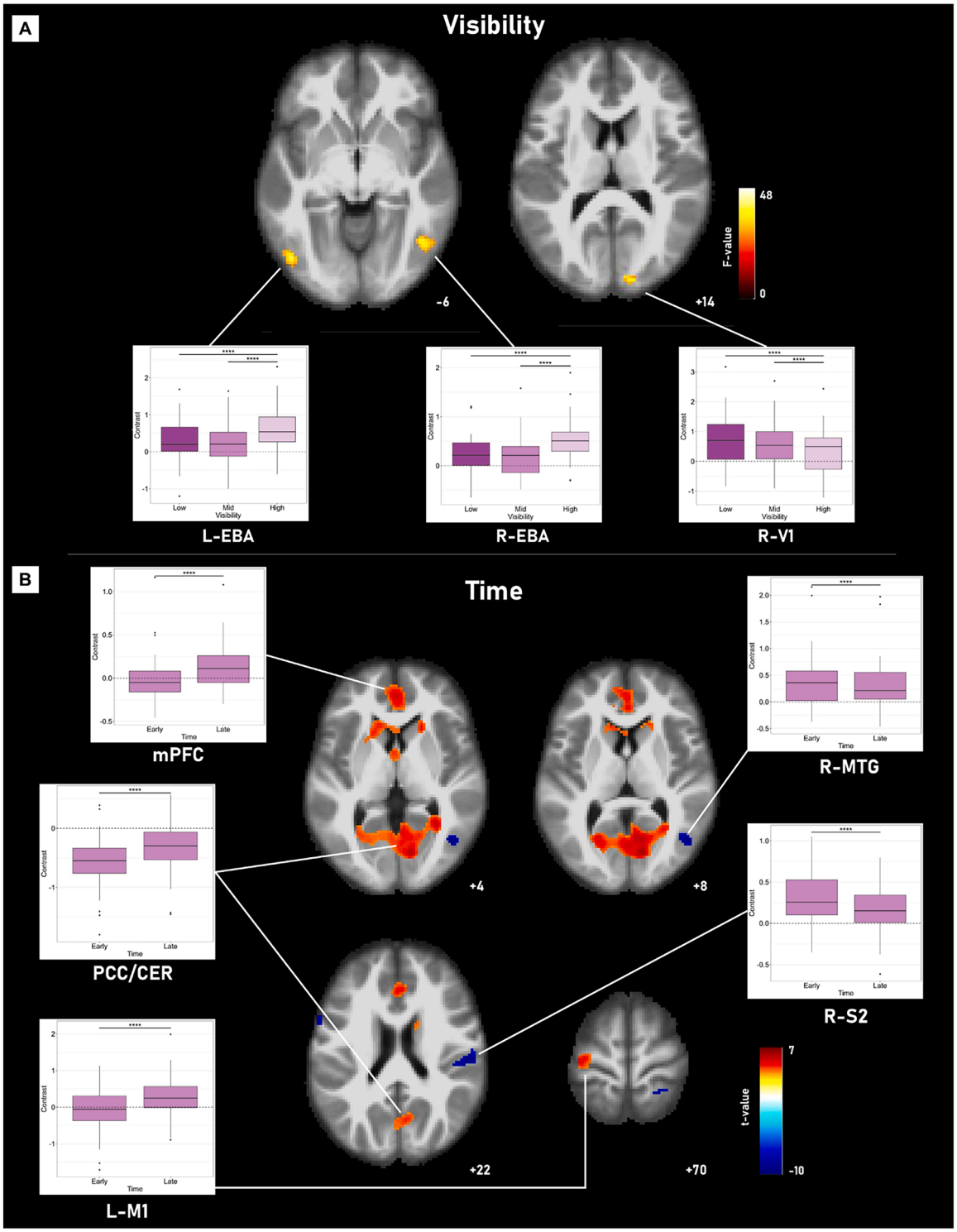

Fig. 6. Whole-brain analysis of the VHI phase. Significant clusters of main effect of Visibility and (A) Time (B) on activation, following a repeated-measures whole-brain ANOVA for Model1/VHI (visuo-tactile stimulation period). Plots represent the activation estimate as a function of factors for each significant cluster of the main effect of Visibility (A) and the five largest clusters for the main effect of Time (B). Dark, medium, and light colors represent low, medium, and high visibility, respectively. Asterisks represent significant differences in post-hoc analysis corrected for multiple comparisons using the Šidák correction (****$p < 0.0001$). Abbreviations correspond to those of Fig. 4.

during the VHI period was not associated with activity in any of the preselected ROIs (all $p_s > 0.05$).

3.4.2. *Model2/Vicariousness*

3.4.2.7. ROI analysis. Using linear mixed-effects models, we analyzed activation differences in the preselected ROIs during the vicarious pain period and with the factors Visibility, Stimulation, and Illusion. The interaction between Visibility and Stimulation on activation was significant only in the left hemisphere, comprising L-V1 [$F(2974) = 4.40$, $p = 0.04$], L-LING [$F(2973) = 4.47$, $p = 0.04$], L-S1 [$F(2976) = 4.61$, $p = 0.04$], L-INS [$F(2975) = 5.12$, $p = 0.04$], L-M1 [$F(2976) = 5.66$, $p =$

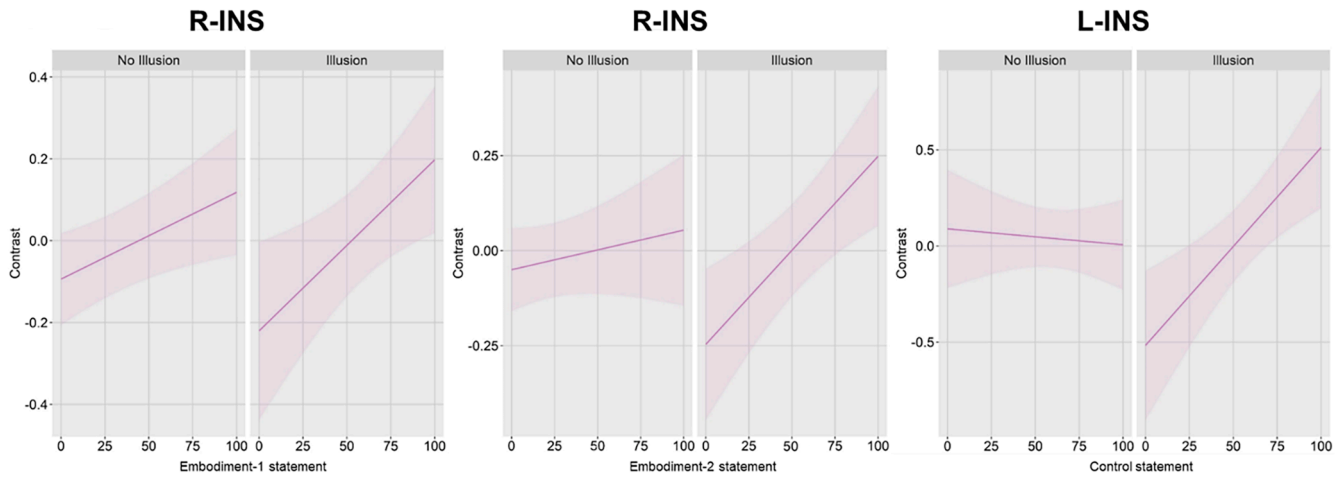

Fig. 7. Brain-perception correlation. activity in the anterior insula was associated with rating on all VHI Statements during the late phase of visuo-tactile stimulation (Model1/VHI). In particular, the activity in the right anterior insula (R-INS) was associated with ratings for Embodiment-1 (left plot) and Embodiment-2 (middle plot) statements. Activity in the left anterior insula (L-INS) was associated with ratings for the Control statement only when participants perceived the illusion (right plot).

0.04], and L-PMC [F(2975) = 5.03, p = 0.04] (Figs. 8, 4). Post-hoc analysis revealed that, following the high visibility condition, the activation of L-M1 and L-PMC during vicarious pain was higher after the synchronous than asynchronous visuo-tactile stimulation (Fig. 8A; yellow in Fig. 4). Similarly, following the medium visibility condition, the activation of L-LING related to vicarious pain was higher after synchronous than asynchronous visuo-tactile stimulation (Fig. 8A; orange in Fig. 4). Conversely, following low visibility condition, in L-V1 the activity related to vicarious pain was lower after synchronous than asynchronous visuo-tactile stimulation (Fig. 8A; brown in Fig. 4). Other pairwise comparisons indicated that after asynchronous visuo-tactile stimulation the activation during the vicarious pain period was lower when preceded by the high visibility condition compared to medium visibility (L-PMC, L-M1, L-INS, and L-S1) (Fig. 8A; black in Fig. 4) and low visibility (L-S1) (Fig. 8A; gray in Fig. 4).

The 3-way interaction between Visibility, Stimulation, and Illusion was significant for the activations of the L-PMC [F(2981) = 5.50, p = 0.04], R-PMC [F(2983) = 5.14, p = 0.04], and R-FBA [F(2980) = 6.39, p = 0.04] (Fig. 8B; white in Fig. 4) during the vicarious pain period. For these three ROIs, when participants perceived the illusion, the activation after synchronous visuo-tactile stimulation was higher following the medium compared to low visibility. In addition, when participants perceived the illusion in the low visibility condition, the activation was lower after synchronous than asynchronous visuo-tactile stimulation. When participants did not perceive the illusion, the activation in L-PMC and R-FBA after asynchronous visuo-tactile stimulation was lower following high than medium visibility. Effect sizes, t-values, and p-values of these significant pairwise differences in post-hoc analyses are reported in Table S5.

3.4.2.8. Whole-brain analysis. The influence of Visibility and Stimulation on the whole brain activity during the vicarious pain period was analyzed through a repeated-measures ANOVA (voxel threshold of unc. $p < 0.001$). The main effect of Visibility (unc. $p < 0.005$) was significant in R-EBA (coordinates: 50, −66, −2; cluster size = 26 voxels), L-EBA (coordinates: −46, −74, −2; cluster size = 23 voxels), and L-V1 (coordinates: −14, −98, 0; cluster size = 57 voxels; Figs. 9A, 4). Post-hoc analysis revealed that the activation was higher for high visibility compared to medium and low in L-V1, but it was lower for high compared to medium and low visibility in L-EBA and R-EBA (Table S6; Figs. 9A, 4). No significant activation clusters were found for the main effect of Stimulation. The analysis also revealed a significant interaction between Visibility and Stimulation in L-M1 (coordinates: −28, −18, 52; cluster size = 20 voxels). Post-hoc analysis of L-M1 activity revealed that in high visibility the activation was higher after synchronous than asynchronous visuo-tactile stimulation (Figs. 9B, 4). This pattern was the opposite in low visibility, where the activation after synchronous visuo-tactile stimulation was lower than after asynchronous visuo-tactile stimulation. Effect-sizes, t-values, and p-values of these significant pairwise differences in post-hoc analyses are reported in Table S6.

3.4.2.9. Brain-perception correlation. Activity in left anterior insula during the vicarious pain was associated with main effect of Illusion (F(1994) = 5.65, p = 0.029) (Fig. S3, Table S6). We observed that activity in this region was lower for trials in which illusion was indicated compared to no indicated illusion. Furthermore, the estimate of skin conductance response to vicarious pain was not associated with activity in any of preselected ROIs (all $p_s > 0.05$) during vicarious pain.

4. Discussion

We investigated how manipulations of visual input influence (i) neural and subjective responses to illusory body ownership (VHI), and (ii) the brain and peripheral activity associated with VHI-related vicarious pain. Body ownership was manipulated through the VHI procedure, providing participants with robotically-controlled tactile stimulation of their hand (tactile stroking) and video-edited visual stimulation of a virtual hand (visual stroking). The visual input of the VHI procedure was manipulated by masking only the virtual hand (low, medium, and high visibility), not the virtual brush. The fMRI analyses showed four main points. First, during the VHI phase (i) manipulating visibility modulated brain activity in visual (bilateral V1 and FBA) somatosensory (L-SMG and R-S1), and multisensory (R-IPS) regions (light and dark blue in Fig. 4), (ii) the activity of visual (R-FBA) and somatosensory (R-S1) regions was higher when visual and tactile stimulations were synchronous (red in Fig. 4), and (iii) the brain activity in visual (L- and R-LING) somatosensory (R-S1, R-S2, L-SMG) and motor (L-M1, mPFC) regions was sensitive to the time of visuo-tactile stimulation (purple and pink in Fig. 4). Second, during the VHI-related vicarious pain, the interaction between visibility and visuo-tactile synchrony influenced the activity of visual (L-V1, R-FBA, L-LING, L-EBA, R-EBA) sensory (L-S1, L-INS) and motor regions (L-M1, L-PMC, R-PMC) (yellow, orange, brown, black, grey, and white in Fig. 4). Third, the time of visuo-tactile stimulation influenced some components of the default mode network (PCC and mPFC), in addition to visual and motor regions. Fourth, subjective ratings of illusory ownership were correlated with brain activity in the

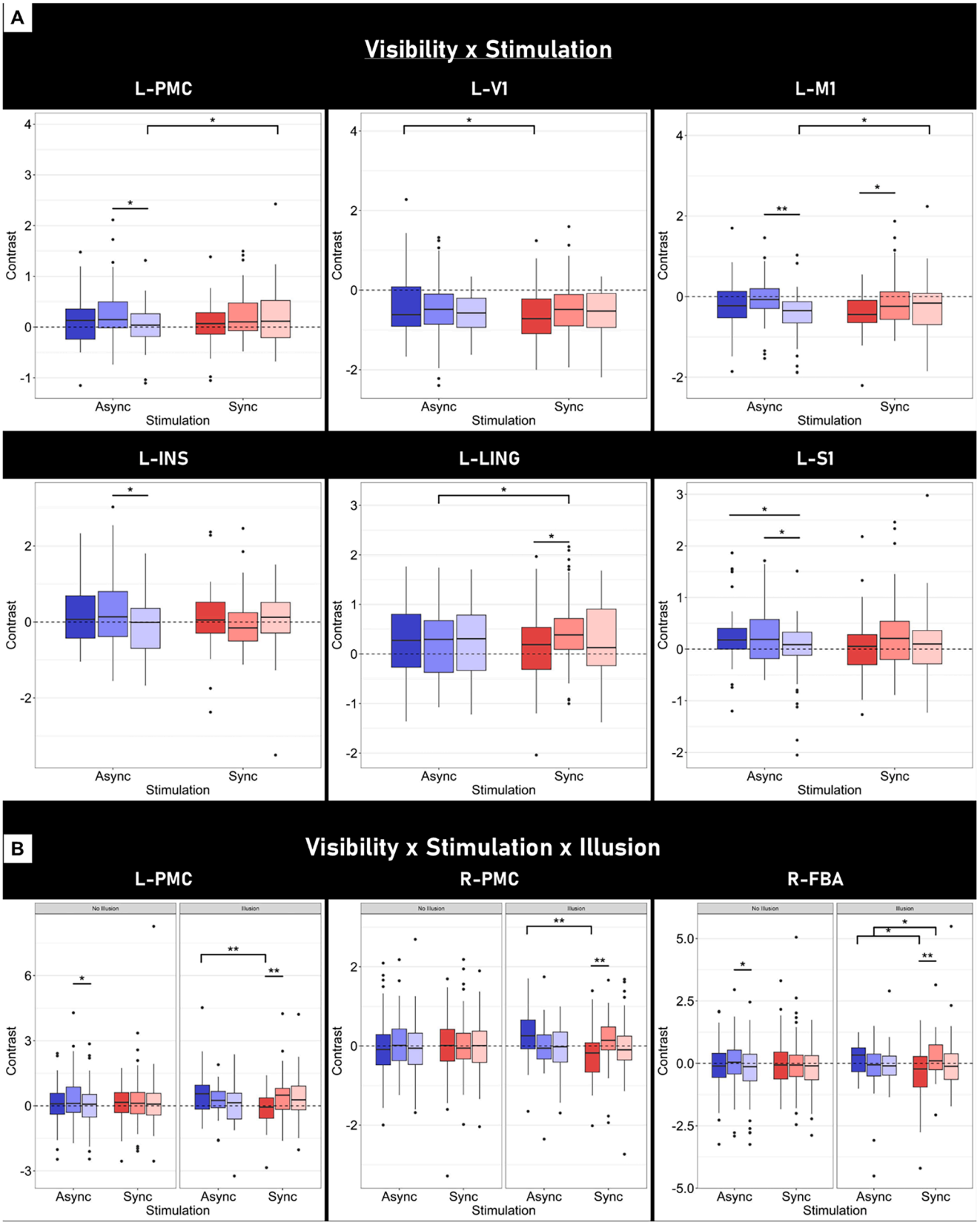

Fig. 8. ROI analysis of the vicariousness phase. Contrast differences in ROIs with significant 2- and 3-way interactions between Visibility, Stimulation, and Illusion on brain activity during the vicarious pain phase. Asterisks represent significant differences in post-hoc analysis corrected for multiple comparisons using Šidák's correction (****$p < 0.0001$, ***$p < 0.001$, **$p < 0.01$, *$p < 0.05$). Abbreviations correspond to those of Fig. 4.

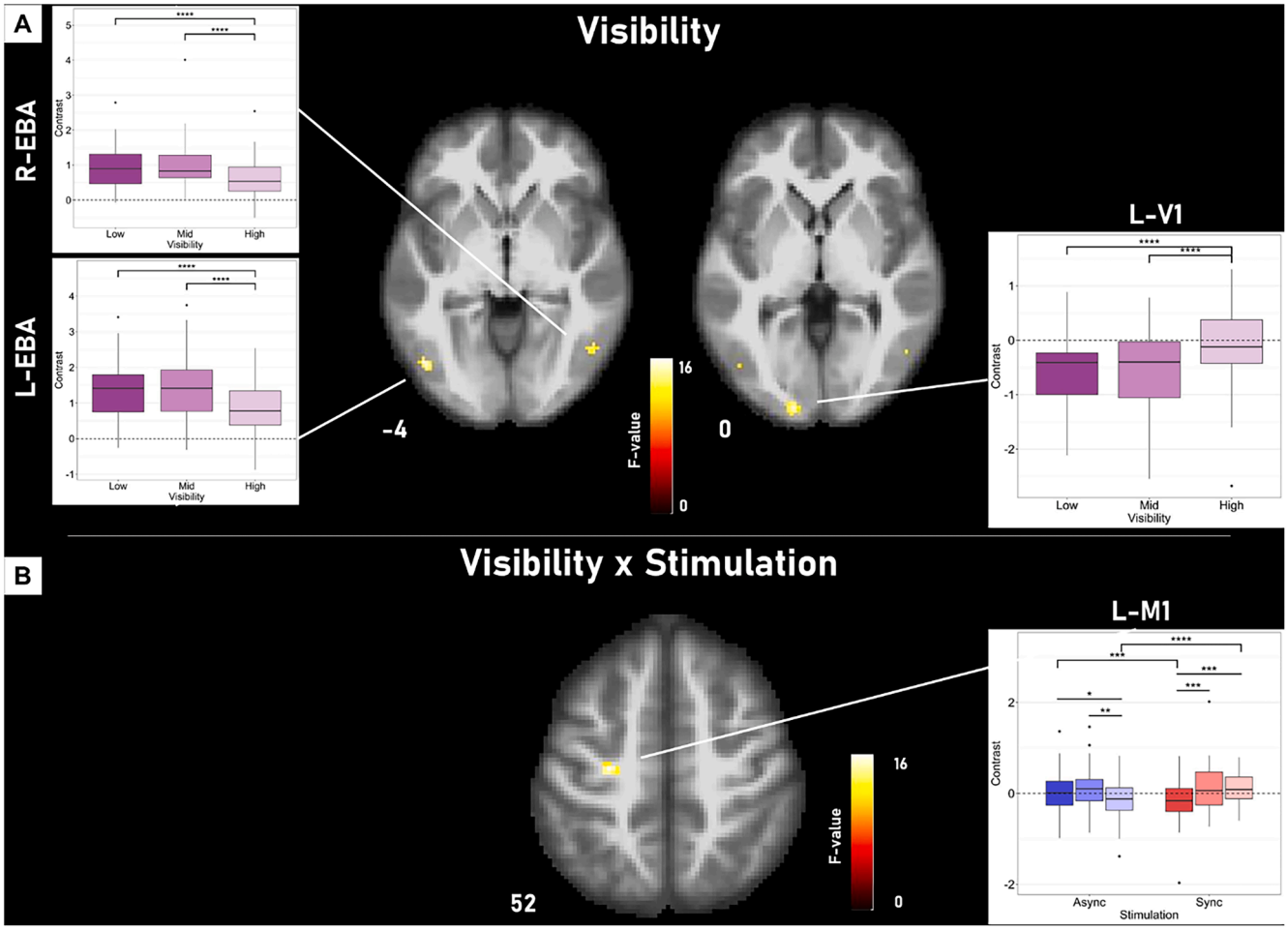

Fig. 9. Whole-brain analysis of the Vicariousness phase. Significant clusters of main effect of Visibility (A) and the interaction between Visibility and Stimulation (B) on activation, following a repeated-measures whole-brain ANOVA for Model2/Vicariousness (vicarious pain phase). Plots represent the activation estimate as a function of factors for each significant cluster of the main effect of Visibility (A) and the Visibility by Stimulation interaction (B). Dark, medium, and light colors represent low, medium, and high visibility, respectively. Asterisks represent significant differences in post-hoc analysis corrected for multiple comparisons using the Šidák correction (****$p < 0.0001$). Abbreviations correspond to those of Fig. 4.

insula.

4.1. *Subjective and objective measures associated with illusory body ownership*

The effects of Visibility manipulations specifically influenced the subjective ratings related to embodiment (Embodiment-1 and Embodiment-2 statements) and did not impact other aspects of the illusion (Control statement). Compared to asynchronous visuo-tactile stimulation, after synchronous stimulation participants provided higher ratings for all statements and perceived the illusion more often (Fig. 3A). The proportion of non-responders in our study (26.7 %) was similar to previous ones (23–28 % as in Bekrater-Bodmann et al., 2014; Ehrsson et al., 2004; Kalckert and Ehrsson, 2014a). The onset time of the perceived illusion did not differ between experimental conditions (Fig. S1). In addition, visuo-tactile stimulation led to higher skin conductance responses when the illusion was perceived (Fig. 3B), but there was no significant overall association between skin conductance and subjective ratings. Confirming that subjective and objective measurements of illusory ownership can be dissociated (Gallagher et al., 2021; Pamplona et al., 2022a; Rohde et al., 2011), our findings extend previous work by showing that manipulating the visual aspects of the dummy hand can influence subjective rather than objective measures of illusory body ownership. One possible interpretation for such a dissociation is that these two types of measurements address different processes, possibly in combination with a higher sensitivity of subjective measures to visibility manipulations compared to objective ones.

Illusory body ownership in RHI setting consists of a proprioceptive distortion, induced by synchronous visuo-tactile stimulation of the actual and dummy limbs, despite their proprioceptive incongruence. During illusory experience, the proprioceptive signals are "overpowered" by incoming visual information, which is generally more reliable for spatial and temporal self-assessment of visuo-tactile stimulation. In other words, the brain resolves the visuo-tactile incongruence by giving more weight to vision than proprioception (Ernst and Bülthoff, 2004). The phenomenology and mental processes involved in such a proprioceptive recalibration can be better understood by modulating the experimental setup parameters. Several studies have investigated the behavioral and neural effects of gradual changes in the coherence of visuo-tactile stimulation (Bekrater-Bodmann et al., 2014; Shimada et al., 2009), but modulating the visibility of only the dummy limb in RHI settings is challenging. Although transparency can be used to manipulate illusory ownership of limbs through a visual channel (Martini et al., 2015; Matsumuro et al., 2022), conditions with different levels of transparency would result in uncontrolled conditions in terms of visual content. Our setup allowed for such visual modulation while keeping uniform other visual factors, i.e. unchanged visibility of the robotic manipulandum, color composition, and brightness. We observed that

the rating of the Embodiment-1 and Embodiment-2 statements and the proportion of perceived illusions were higher for high then medium and low visibility. We observed larger effect sizes were observed for the rating of Embodiment-2 statement (visual aspects of embodiment), compared to the rating of the Embodiment-1 statement (proprioceptive aspects of embodiment). Furthermore, we observed that the visibility-related increase in the rating of Embodiment-2 statement was more pronounced for synchronous visuo-tactile stimulation (Fig. 2), in line with a previous study on limb transparency in RHI setups (Okumura et al., 2020). These results advocate a multisensory integration of visual and tactile aspects in the VHI experiment. While enhanced visibility and synchronous visuo-tactile stimulation separately led to increased illusory ownership, their effects were cumulative for the illusory experience. The relationship between visibility and illusory ownership is consistent with behavioral evidence from studies that modulated limb visibility through transparency manipulations (Martini et al., 2015; Matsumuro et al., 2022). Our results seem to oppose to those of a study associating a higher rating of illusory ownership with higher noise in participants' field of view (i.e., degraded visibility; Chancel et al., 2022). However, the visibility manipulations of Chancel et al. (visual noise) changed the visual parameters of the different experimental conditions and affected the entire field of view of the participant. This approach changes the quality of the visual input of the different experimental conditions and increases the visual uncertainty of the entire scene, including the exact location of the stroke on the dummy hand as well as the stroking object. Conversely, in our and others' setups (Martini et al., 2015; Matsumuro et al., 2022), the visibility degradation only affected the visual uncertainty of the dummy limb (not the whole scene), whereas the stroking location and object were not affected. Thus, in our study, visibility-dependent ownership can be explained by top-down processing of the correspondence between virtual and actual hands. Furthermore, we argue that the degraded visibility affecting illusory ownership in our experiment also differs from a setting in which there was no visual input at all from a limb, such as the proposed "invisible hand" illusion (Guterstam et al., 2013) or the somatic RHI (Ehrsson et al., 2005). In these experimental setups, visualization of the limb was removed, whereas we modulated visibility without completely removing the visual stimulus. In sum, altering the visual parameters of the experimental conditions or the entire visual field – such as through transparency, visual noise, or limb visualization – may address different phenomenological aspects compared to our study. For example, a semi-transparent dummy hand might evoke an illusion of owning a peculiar transparent body, whereas crystallizing the dummy hand could disrupt the illusion altogether. Based on this, we conclude that the visibility manipulations of the dummy hand in our study specifically influenced the subjective aspects of illusory ownership.

Interestingly, for late experimental runs compared to early runs (Fig. 2), we observed that participants rated illusory ownership higher for Embodiment-1 and Embodiment-2 statements and indicated a higher proportion of perceived illusions, consistent with previous findings (Fuchs et al., 2016). Illusory ownership is thought to be associated with reduced attention to sensory signals derived from the limb (Riemer et al., 2019). Given that our experimental runs lasted more than 10 min, we speculate that participants may have reduced their attention throughout the runs, which was beneficial for proprioceptive recalibration. In other words, it is reasonable that participants' stronger attentional focus on visuo-tactile signals in early phases of the stimulation reduced the likelihood of illusory ownership. Conversely, a possible weaker focus (and/or greater fatigue) during the late phases of stimulation increased the likelihood of illusory ownership. An alternative explanation is that the prolonged exposure to an image of a hand, regardless of its high or low visibility, may have simply been perceived by participants as an embodied object. In any case, our results suggest that habituation to the experimental protocol may be beneficial rather than detrimental for inducing illusory ownership. In addition to attentional effort and the gradual embodiment switch, other mental states, such as fatigue, engagement, or motivation, could also be involved in this phenomenon. However, we lack data on any of these factors to draw conclusions, and the mechanism behind this effect remains uncertain. Although the influence of stimulation timing on the likelihood of illusory ownership requires deeper understanding, it may help future researchers to set prior instructions and design experiments to maximize the chances of inducing illusion.

4.2. *Differential activity modulated by visibility of virtual hand during visuo-tactile stimulation*

We found that the activity of visual, somatosensory, and multisensory regions was differentially modulated by visibility conditions during visuo-tactile stimulation. Some visual regions (such as bilateral V1, EBA, and FBA) were more active when the virtual hand was clearly visible (high) compared to degraded visibility conditions (medium and low) (Fig. 4). EBA (Downing et al., 2001; Urgesi et al., 2004) and FBA (Kitada et al., 2009; Peelen and Downing, 2005) are usually linked to the observation of human bodies. Nevertheless, both EBA (Arzy et al., 2006; Bekrater-Bodmann et al., 2014; Ionta et al., 2014; Limanowski et al., 2014b) and FBA (Nilsson and Kalckert, 2021) have also been associated with illusory body ownership. We propose that our experimental setup activated EBA and FBA because participants were observing a human body, which was better perceived in the high visibility condition. The visual cortex showed the opposite pattern: its activity was lower at high visibility compared to other levels (Figs. 4, S2B, and C). Higher activity in V1 has been associated with lower levels of visibility, reflecting greater effort to process scrambled compared to intact images (Coggan et al., 2017) and higher processing in the ventral visual pathway to make sense of the image. In addition, we observed greater activity in somatosensory regions (R-S1, R-IPS, and L-SMG) for high than low/-visibility during visuo-tactile stimulation (Fig. 4). Neural activity in S1 encodes somatosensory input from the contralateral limb (Chen et al., 2008; Kanayama et al., 2007, 2009), is associated with illusory body ownership (Sakamoto and Ifuku, 2021), and can modulate the strength of RHI (Hornburger et al., 2019). The IPS has been associated with top-down attention (Corbetta et al., 2002; Ehrsson et al., 2004; Gentile et al., 2011; Tsakiris, 2010), which may be elicited by visualization of well-defined body parts and associated with proprioceptive recalibration (Ehrsson et al., 2005; Limanowski and Blankenburg, 2015a; Shimada et al., 2009). The SMG has been associated with illusory embodiment of a dummy limb (Brozzoli et al., 2012; Limanowski and Blankenburg, 2015b), with the representation of peripersonal limb space (Brozzoli et al., 2011), and is differentially activated by visual and tactile inputs related to body representation (Pamplona et al., 2022b). Notably, we observed a contralateral IPS response to the visualization of a left hand, consistent with a previous finding (Zopf and Williams, 2013). Overall, we propose that decreasing the visibility of the dummy hand reduced the activity of S1 (inducing a weaker illusion), IPS (weakening proprioceptive recalibrations), and SMG (minimizing the embodiment of the dummy hand).

4.3. *Differential activity modulated by synchrony of visuo-tactile stimulation*

Activation of SMA was modulated by the interaction between Stimulation and Illusion, in that it was higher during synchronous than asynchronous visuo-tactile stimulation, specifically when subjects perceived the illusion (Fig. 5D). This finding provides evidence that the SMA acts upon coupling coherent visual and tactile sensory signals during conscious illusory embodiment of the dummy limb. Because these differences in SMA activity were bound to the visuo-tactile stimulation period, independent of the vicarious pain period, the possible interpretation that this activity reflects inhibition of the defensive response (Ehrsson, 2007) can be excluded. Although the SMA is not one of the most reported regions linked to RHI, previous work has

nevertheless shown that it is involved in illusory body ownership (Abdulkarim et al., 2023; Brusa et al., 2023; Limanowski et al., 2014b; Pyasik et al., 2019). We extend this knowledge by showing that SMA activation accounts for visibility, but only when the illusion is consciously perceived. This finding demonstrates that top-down cognitive states related to illusion perception can shape neural response to bottom-up multisensory input.

Activity in R-FBA and R-S1 depended on the coherence of the visuo-tactile stimulation, since activity was higher during synchronous compared to asynchronous visuo-tactile stimulation (Fig. 5B). Activity in these regions was also modulated by visibility conditions, indicating their multisensory nature. FBA has previously been associated with body ownership in studies using RHI-based experimental setups (Nilsson and Kalckert, 2021). Differential activity in S1 due to coherent levels of visuo-tactile stimulation is not a ubiquitous finding in RHI-based studies (Limanowski et al., 2014b), but was here associated with illusory ownership.

4.4. Activity modulated over time during visuo-tactile stimulation

In some brain regions, activation was different between the first and second half of the visuo-tactile stimulation (Fig. 5C). This difference allows to infer how activity evolved over time during the illusion induction phase, as changes in neural activity over time would be caused by the increase in illusory ownership. Several studies have found that objective (Botvinick and Cohen, 1998; Gallagher et al., 2021; Rohde et al., 2011; Tsakiris and Haggard, 2005) and subjective (Fuchs et al., 2016) measures of RHI increase over time. A simple explanation for the increase in illusory ownership over time was proposed by Gallagher et al. (2021), who suggested that a longer period of synchronous visuo-tactile stimulation provides participants with more opportunities to establish a proprioceptive connection with the dummy limb. In our experiment, the median time to the illusion onset was in the first half of the visuo-tactile stimulation period (Fig. S1). However, it is thought that the level of illusory ownership should increase after this first temporal window of coherent visual and tactile input, which lasts until the illusion is perceived (Riemer et al., 2019). Therefore, as shown in previous studies, the level of illusory ownership should be higher in the second compared to the first half of visuo-tactile stimulation. This pattern would be reflected in several time-related changes in brain activity. In fact, activity decreased over time in L-SMG, R-S1, R-S2, and R-MTG (Figs. 5C and 6B, Tables S2 and S3). Previously, it has been proposed that activity in these temporo-parietal embodiment-related regions would increase during visuo-tactile stimulation, possibly due to proprioceptive recalibration and resolution of multisensory conflict (Ehrsson et al., 2004; Limanowski et al., 2014b). Here, our time-related findings support an alternative interpretation, in which brain activity decreases over time due to loss of ownership (or deafference) of the actual hand (Longo et al., 2008a) associated with the emergence of illusory ownership of the dummy hand.

In contrast, activity increased over time in L-M1, bilateral LING, and default mode regions (mPFC and PCC) (Figs. 5C and 6B). Since motor activations usually follow contralateral inhibition (Allison et al., 2000), it is possible that the temporal increase in L-M1 activity, [ipsilateral to the (left) dummy hand] is an epiphenomenon of inhibition in the contralateral (right) motor regions due to a stronger illusion and deafference. Furthermore, activations of the lingual cortex have been associated with third-person perspective taking (Jackson et al., 2006), which implies a detachment from one's own (first-person) body. In the present study, lingual regions were more active in the late phases of visuo-tactile stimulation, suggesting that these phases would be associated with greater third-person perspective taking. This would also be consistent with previous evidence that visual regions are sensitive to illusory body ownership (Limanowski et al., 2014a). Finally, the time-related increase in default mode activity (mPFC, PCC) can be explained by an increase in the incidence of task-unrelated and internally-oriented thoughts, as well as self-localization in space and interoceptive sensitivity (Andrews-Hanna et al., 2014).

4.5. Association of activity and subjective rating during visuo-tactile stimulation

Subjective ratings for the Embodiment-1 and Embodiment-2 statements were positively correlated with brain activity in the bilateral insula during the late phase of visuo-tactile stimulation (Fig. 7), independent of the perceived illusion. This similarity can be explained by the fact that both statements concern embodiment, although they focus on the tactile and visual aspects of illusory ownership, respectively. Ratings for the Control statement (which reflect affective aspects, not embodiment) were associated with insular activity too, but only during consciously perceived illusion, possibly due to self/other discrimination processing (Ehrsson et al., 2007a). The correlation between embodiment ratings and insular activity supports that the anterior insula plays an important role in the subjective evaluation of illusory aspects of ownership. The insular cortex has been associated with body ownership in experiments based on RHI settings (Ehrsson et al., 2007a), as well as with the integration of interoceptive information and the sense of agency (Singer et al., 2004; Tsakiris, 2010; Tsakiris et al., 2007). Interestingly, with the neutral rating point as a reference (converted to a value of "50″), negative and positive ratings were associated with deactivation and activation, respectively, of the insular cortex during the illusory experience (Fig. 6), suggesting that this region is unidimensionally modulated according to the valence of the illusory experience. A recent meta-analytic study suggested that the insula is not directly involved in proprioceptive recalibration during RHI experience (Nilsson and Kalckert, 2021). Our study endorses this idea by demonstrating that the insula is not involved in the embodiment process per se (Gallagher et al., 2021), but rather in the accessory, ongoing subjective evaluation of the illusory experience, reflecting the complex nature of the RHI experience.

4.6. Differential activity during vicarious pain

To neurally assess whether the virtual hand was actually embodied by participants, we recorded brain activity during vicarious pain targeting the virtual hand after visuo-tactile stimulation. This approach allows to assess whether brain responses differ as a function of Visibility and Stimulation. In addition, our analysis included the participants' indication of illusion perception, a measure of conscious perception of body ownership. We observed a significant interaction between Visibility, Stimulation, and Illusion on the activation of bilateral L-PMC, R-PMC, and R-FBA (Fig. 8B). Furthermore, the interaction Visibility x Stimulation was significant for the activity of a set of regions located in the left hemisphere, ipsilateral to the virtual and participants' hands (L-INS, L-PMC, L-V1, L-M1, L-LING, L-S1) (Fig. 9A).

First, there were more condition-related significant differences in brain responses to vicarious pain when participants consciously perceived the illusion compared to when they did not perceive it (right facets of the graphs in Fig. 8B). These findings demonstrate the importance of including perceived illusion as a factor in the study of neural differences due to illusory embodiment.

Second, during vicarious pain, after synchronous visuo-tactile stimulation, and when the illusion was perceived, the response in the bilateral PMC and FBA was higher for medium compared to other visibility levels (middle red boxplots in the right facet of Fig. 9B). Previous literature on visibility modulation and embodiment indicates that pain ratings in healthy and clinical populations are lower when a limb is presented in medium visibility compared to good or poor visibility conditions (Matamala-Gomez et al., 2019; Matsumuro et al., 2022). In fact, degraded visibility reduced the sense of ownership (Fig. 2), which has been suggested to increase tolerance to painful stimuli (Martini et al., 2015). On this basis, we propose that the higher activity for an

intermediate visibility level may lead to a higher pain threshold compared to other visibility levels. Our results suggest that neural activity during vicarious pain is related to the uncertainty in embodying the virtual hand in an ambiguous visibility condition, whereas illusory embodiment is more likely to occur in high or low visibility conditions (Guterstam et al., 2013). This uncertainty in the embodiment process may have partially counteracted the illusory ownership previously induced by the synchronous stimulation in our protocol.

Third, during vicarious pain, after asynchronous visuo-tactile stimulation, and when the illusion was perceived, the response in the bilateral PMC and FBA was greater for low compared to the other visibility levels (left blue boxplots in the right facet of Fig. 9B). Accumulating evidence suggests that asynchronous visuo-tactile input, rather than simply not leading to illusory ownership, acts in the opposite direction, diminishing the sense of ownership that would be induced by only viewing the dummy limb (Riemer et al., 2019). For example, weaker or negative proprioceptive drifts have been reported for asynchronous visuo-tactile stimulation compared to visual presentation of the limb or baseline ratings (Fuchs et al., 2016; Kalckert and Ehrsson, 2014b; Riemer et al., 2013; Rohde et al., 2011). Therefore, while experimentally controlling for the weight of visuo-tactile input during stimulation, there is evidence that asynchronous stimulation may rather induce disembodiment of the dummy limb (Riemer et al., 2019), which may also have been observed in our results. Thus, consistent with the situation described in the previous paragraph, brain processes related to a higher pain threshold were more likely to occur toward a disembodied virtual hand, induced by the experimental conditions.

Interestingly, during vicarious pain, EBA activity in response to aversive visual stimulation was lower when the preceding visuo-tactile stimulation displayed a virtual hand in high visibility compared to other levels. Because embodiment processes were induced during the visuo-tactile stimulation when the virtual hand was displayed in high visibility (Fig. 4), the lower EBA activity during vicarious pain suggests an attempt to dissociate the embodied virtual hand and pain avoidance (Pamplona et al., 2022c). In other words, participants may have attempted to avoid the noxious experience of a once embodied virtual hand, and this process was reflected in lower EBA activity. Conversely, during vicarious pain, V1 activity was more negative when the preceding visuo-tactile stimulation displayed a virtual hand in low visibility compared to other levels (Fig. 4A). The increased activity in early visual areas during visuo-tactile stimulation in response to viewing the virtual hand in low visibility may have led to greater V1 adaptation during subsequent vicarious pain.

4.7. Multisensory brain regions during visuo-tactile stimulation

We investigated the weight of vision on neural processes related to illusory body ownership. Subjective measures showed that both visibility and coherence of the visuo-tactile stimulation positively influenced the sense of embodiment in our setup (Figs. 2 and 3A). As a corollary to this finding, we also observed that the highest level of subjective embodiment was achieved when optimal visibility and coherent visuo-tactile stimulation were combined (see interaction in Fig. 2B). This finding not only endorses the explanation that proprioceptive recalibration is generated by a spatial congruence of visual and tactile inputs, but also shows that modulating the intensity of these sensory inputs influences the resulting illusory embodiment. By comparing the effect sizes of visual and tactile modulations (Table S1), we argue that the coherence of the visuo-tactile stimulation has a greater weight on the final illusory ownership than vision alone. Nevertheless, we reiterate that modulation of both factors influences proprioceptive recalibration.

Although illusory ownership is thought to arise as a multisensory integration of a multitude of brain regions (Bekrater-Bodmann et al., 2014; De Castro and Barbosa Gomes, 2017), we observed that two specific brain regions are key to the modulation and integration of visual and tactile stimulation: the (contralateral) R-S1 and R-FBA (Fig. 4). These regions showed lower activity for medium compared to high visibility (Fig. 5A), as well as higher activity for synchronous compared to asynchronous visuo-tactile stimulation (Fig. 5B). In addition, R-S1 also showed lower activity during a late compared to an early phase of visuo-tactile stimulation (Fig. 5C), which is thought to be due to a relative proprioceptive recalibration that occurs during the early stages of stimulation. S1 has previously been associated with body ownership and with changes in its topographic representation during illusory ownership (Kanayama et al., 2007; 2009; Schaefer et al., 2009). Furthermore, S1 has been found to be more strongly connected with EBA during synchronous compared to asynchronous visuo-tactile stimulation (Limanowski et al., 2014b), integrating visual representation with somatosensory information of body parts and building self-identification with a body (Ionta et al., 2011). The FBA (Schwarzlose et al., 2005) responds selectively to body parts (Kitada et al., 2009; Peelen and Downing, 2005). Activity in the FBA modulated by visuo-tactile stimulation may be related to the identification of a body part as one's own. We propose that S1 encodes somatosensory aspects of illusory body ownership, which would be further modulated by the visibility of the dummy hand and the duration of the visuo-tactile stroking, whereas FBA would be rather implicated in the visual aspects of the illusion, sensitive to the visibility of the dummy hand. Other regions found in the present study are considered to be part of distinct networks that support changes in sensory inputs.

Regions commonly reported to be associated with illusory ownership, such as the premotor cortex, intraparietal sulcus, and insula (Bekrater-Bodmann et al., 2014; Ehrsson et al., 2004; Nilsson and Kalckert, 2021), were not influenced by visibility manipulations during visuo-tactile stimulation. This result suggests that these regions are rather involved in other processes related to illusory experience, but not directly involved in the neural processes of proprioceptive recalibration. The discrepancy between our results and previous ones may be due to differences in experimental setup, definition of visibility and visuo-tactile stimulation, and ROI definition. In particular, the results regarding the premotor cortex during visuo-tactile stimulation were also absent in other studies that used an automated setups (Limanowski et al., 2014b; Tsakiris et al., 2007), and it has been argued that the outcome depends on the presence of a human agent during stimulation (Limanowski et al., 2014b). We found that the premotor cortex was present only for vicarious pain, which was indeed provided by a pre-recording showing a human agent. We argue here that the premotor activity in our study was likely evoked by preparation for an observed action (Ehrsson et al., 2005). Finally, a recent and compelling Model2/Vicariousness based on Bayesian concepts has proposed that the modulation of illusory ownership is a result of uncertainty-based probabilistic inference of the dummy limb as a common cause of the visual and somatosensory inputs (Chancel et al., 2022). This Bayesian model does not consider an interplay between online and offline body representations, suggesting that higher-level brain regions are not crucial for producing illusory ownership (Gallagher et al., 2021). This view is consistent with our findings. We propose that future studies could investigate how prior variance of contralateral S1 and FBA activity levels would predict induced embodiment according to this Bayesian model.

4.8. Strengths of the study

Several methodological and analytical features of our study allowed us to assess the weight of vision during illusory body ownership in the brain. First, we used edited videos of hands being stroked to generate visual stimulation to modify only the dummy hand and not the stroking object, keeping the visual content unaltered across conditions. While manipulating the characteristics of tactile stimulation in the RHI setting is relatively easy and well-studied, changing the visibility dimension in this context is more challenging. In a standard RHI setup, changes in the

visibility of the hand typically also modify the stroking object, and degrading the visibility of the participant's entire field of view may impair illusory ownership.

Second, the robotic setup conferred spatial and temporal precision to the tactile stimulation and avoided eventual biases in brain responses due to the presence of and interaction with a person during the illusion experience. The predetermined trajectories on the MR-compatible robot were designed to provide participants with affective velocities and irregular trajectories – which should induce higher levels of illusion –, while controlling for movement in synchronous and asynchronous stimulations. The trajectories of tactile stimulation would be challenging for a human to deliver with spatial and temporal accuracy. Moreover, it has been suggested that the mere visualization of human actions may interfere with the processing of self-related information (Limanowski et al., 2014b). Therefore, the use of a robotic system contributed to ensuring optimal conditions for studying illusory body ownership.

Third, in our skin conductance and ROI analyses, we included trial-specific indication of perceived illusion as a factor that could influence the dependent variable, rather than removing data from non-responders. The common practice of removing non-responders may ultimately remove relevant variance, affect comparability across experiments, and bias results depending on the criteria used (Riemer et al., 2019). In fact, because participants rated the statements on each trial, each value was associated with a neural or physiological response in the linear mixed-effects model. In some of our results, distinct patterns emerged when we analyzed trials with and without indication of perceived illusion (e.g., Figs. 5 and 7). Although applying linear mixed-effects models to whole-brain analysis is currently challenging, our ROI analyses showed that separating trials with and without perceived illusion is highly beneficial for studying illusory ownership.

4.9. Limitations

First, only three visibility levels were considered. For a broader understanding of the weight of vision on the neural processes of illusory body ownership, more visibility levels would be required. For example, our results suggest that levels between high and medium visibilities could lead to intermediate illusory states. In fact, our results on brain responses during vicarious pain suggest that medium visibility during visuo-tactile stimulation has a peculiar effect on illusory limb ownership, that has previously been linked to analgesia (Matsumuro et al., 2022). More visibility levels available during visuo-tactile stimulation would help determine optimal effects. However, more visibility levels would mean more trials, longer scanning times, and a consequent loss of subject compliance. Future studies aimed at further investigating neural responses of illusory ownership due to visibility could isolate factors of interest to optimize measurements and even analyze visibility levels parametrically (Schröder et al., 2019).

Second, we collected no data on how subjective illusory ownership changed over the course of the visuo-tactile stimulation and the exact time course of illusory ownership in our experiment cannot be determined. Therefore, we could only assume that ownership increased over time based on previous findings (see Section 4.4) and offer a simplistic description of the temporal changes in brain mechanisms. While future studies may address this point, it is important to consider that measuring the subjective illusion over time also influences the illusion itself (Rohde et al., 2011). Moreover, the temporal evolution of the illusory experience is likely to be highly subject- and experiment-specific, and perhaps even an all-or-nothing phenomenon (Chancel et al., 2022; Riemer et al., 2019), which complicates this type of investigation.

Third, our most significant results were obtained using ROI analysis, which may affect comparability across studies (Nilsson and Kalckert, 2021). Of relevance here, this field of study tends to rely on a priori analysis and whole-brain results are relatively scarce (Nilsson and Kalckert, 2021).

Fourth, non-Caucasian skin color was not an exclusion criterion. Variations in skin color may have influenced the illusion induction in some participants due to a potential difference between the color of the virtual hands (recorded from Caucasian individuals) and the specific participant's hand. Since we did not collect data on skin color, we were unable to assess whether this factor impacted our results.

Fifth, it could be argued that the training phase of the experiment might have induced placebo effects related to participants' expectations about the illusion. While we acknowledge that expectations can influence bodily illusions (Lush et al., 2021), we further note that (i) our participants were not told to expect the presence or absence of the illusion in one or another specific condition of visuo-tactile stimulation, and (ii) the evaluation of behavioral and neural differences across conditions should cancel out any potential placebo effects caused by eventual expectation.

Sixth, it could be argued that the Control statement in our study is not a "pure" control statement because it evaluates the affective aspects of the VHI. However, the VHI statements of the present study were selected on the basis of their compatibility with our experimental setup, as well their specificity in measuring only embodiment or other aspects of the VHI. Thus, according to previous psychometric research (Longo et al., 2008b), our Embodiment-1 statement had high embodiment and communalities values both in synchronous and asynchronous stimulation, our Embodiment-2 statement was still related to embodiment, but to a lesser extent (low values in embodiment and communalities), and our Control statement had no links to embodiment, loss of own hand, or movement, having the highest values for affect and communalities. Notably, in our study the Control statement was not correlated with Embodiment-1 and Embodiment-2 statements, constituting a reasonable compromise between the need to control for embodiment aspects and the challenge of finding pure control statements (Riemer et al., 2019).

Seventh, we acknowledge that the visuo-tactile stimulation induced relatively low levels of embodiment based on the subjective ratings. However, despite the moderate levels of subjective ownership during visuo-tactile stimulation, we were still able to find significant differences in subjective illusory ownership across conditions.

5. Conclusions

Here, we characterized the neural processes, as well as subjective and objective measures, related to the sense of embodiment as modulated by visibility, coherence, and time of visuo-tactile stimulation. Not only visual, but also somatosensory regions were influenced by visibility manipulations during visuo-tactile stimulation. In general, degraded visibility decreased activity in these regions. In addition, prolonged exposure to visuo-tactile stimulation increased activity in visual regions, but decreased activity in somatosensory regions. During visuo-tactile stimulation, visual (R-FBA) and somatosensory (R-S1) regions were sensitive to both visibility and synchrony, suggesting a central role of these regions in integrating multisensory inputs in the context of illusory body ownership. The vicariousness phase activated visual (L-V1, L-LING), motor (L-M1, L-PMC, R-PMC), and somatosensory (L-S1, L-INS) regions. The insular and premotor cortices, commonly associated with illusory ownership, were here related to subjective evaluation of the illusory experience. In sum, the present study shows that, although both visibility and visuo-tactile synchrony can independently influence the sense of embodiment, specific responses to a consciously embodied limb arise only when the two features are combined.

We focused painful settings based on previous evidence that the observation of a threatening stimulus delivered to the rubber hand elicits specific cortical responses (Ehrsson et al., 2007b; Heldmann et al., 2024) and skin conductance modulations (Fan et al., 2021; Hagni et al., 2008). Nevertheless, it is worth noting that, beyond pain-related settings, the rubber hand illusion affects many different domains. For instance, specifically after synchronous visuo-tactile stimulation, the premotor cortex is activated by both vicarious pain and touch, but its activation is higher for touch than pain (Pamplona et al., 2022c). Along

this line, it could be possible to hypothesize that variations of the rubber hand's visibility may affect the RHI-related (i) responsiveness of the motor cortex (Golaszewski et al., 2021), (ii) modulation of somatosensory-evoked potentials (Zeller et al., 2015), (iii) influence on cognitive processing such as mental rotation (Ionta et al., 2013) and body awareness (David et al., 2014)".

Future research on the impact of manipulating visual input on brain activity related to illusory body ownership, as revealed by the present study, could explore several directions. One promising avenue is to investigate the temporal dynamics of neural responses using high-resolution techniques like magnetoencephalography and electroencephalography to complement fMRI findings. These studies could help understand whether visibility manipulations affect precise timing of brain activity changes during the induction of body ownership illusions. Further studies could investigate whether individual differences in the rubber hand illusion (Haans et al., 2012) may interact with the susceptibility to visibility manipulations, including age, gender, sensory suggestibility, personality, and cultural background.

Data statement

The data that support the findings of this study are openly available at https://github.com/gustavopamplona/VHI

CRediT authorship contribution statement

Gustavo S.P. Pamplona: Writing – review & editing, Writing – original draft, Methodology, Investigation, Formal analysis, Data curation. **Amedeo Giussani:** Investigation, Data curation. **Lena Salzmann:** Writing – review & editing, Investigation, Data curation. **Philipp Staempfli:** Writing – review & editing, Supervision, Methodology, Investigation. **Stefan Schneller:** Writing – review & editing, Methodology. **Roger Gassert:** Writing – review & editing, Supervision, Methodology. **Silvio Ionta:** Writing – review & editing, Writing – original draft, Validation, Supervision, Project administration, Methodology, Funding acquisition, Data curation, Conceptualization.

Declaration of competing interest

All authors declare no conflicts of interest

Data availability

Data will be made available on request.

Acknowledgments

This work was supported by the Swiss National Science Foundation (Grant PP00P1_202665 / 1 to Silvio Ionta). We thank Prof. Vince Calhoun for the support on maximizing data estimates of brain responses using HRF temporal derivatives, Dr. Julio Dueñas and Dr. Paulo Carvalho for operational assistance with the robot, Dr. Olivier Lambercy and Jaeyong Song for helping with the robot's maintenance, Bruno Kaufmann and Lavinia Albanese for helping with the experimental setup, and Elliott Schnyder for additional assistance with data collection. The data of this study are available at https://github.com/gustavopamplona/VHI.

Supplementary materials

Supplementary material associated with this article can be found, in the online version, at doi:10.1016/j.neuroimage.2024.120870.

References

Abdulkarim, Z., Guterstam, A., Hayatou, Z., Ehrsson, H.H., 2023. Neural substrates of body ownership and agency during voluntary movement. J. Neurosci. 43, 2362–2380.
Allison, J.D., Meador, K.J., Loring, D.W., Figueroa, R.E., Wright, J., 2000. Functional MRI cerebral activation and deactivation during finger movement. Neurology 54, 135. -135.
Andrews-Hanna, J.R., Smallwood, J., Spreng, R.N., 2014. The default network and self-generated thought: component processes, dynamic control, and clinical relevance. Ann. N. Y. Acad. Sci. 1316, 29–52.
Armel, K.C., Ramachandran, V.S., 2003. Projecting sensations to external objects: evidence from skin conductance response. Proc. R. Soc. Lond. Ser. B Biol. Sci. 270, 1499–1506.
Arzy, S., Thut, G., Mohr, C., Michel, C.M., Blanke, O., 2006. Neural basis of embodiment: distinct contributions of temporoparietal junction and extrastriate body area. J. Neurosci. 26, 8074–8081.
Bach, D.R., Friston, K.J., 2013. Model-based analysis of skin conductance responses: towards causal models in psychophysiology. Psychophysiology 50, 15–22.
Bekrater-Bodmann, R., Foell, J., Diers, M., Kamping, S., Rance, M., Kirsch, P., Trojan, J., Fuchs, X., Bach, F., Cakmak, H.K., Maass, H., Flor, H., 2014. The importance of synchrony and temporal order of visual and tactile input for illusory limb ownership experiences - an FMRI study applying virtual reality. PLoS One 9, e87013.
Botvinick, M., Cohen, J., 1998. Rubber hands 'feel' touch that eyes see. Nature 391, 756.
Braithwaite, J.J., Broglia, E., Watson, D.G., 2014. Autonomic emotional responses to the induction of the rubber-hand illusion in those that report anomalous bodily experiences: evidence for specific psychophysiological components associated with illusory body representations. J. Exp. Psychol. Hum. Percept. Perform. 40, 1131.
Brett, M., Anton, J.L., Valabregue, R., Poline, J.B., 2002. Region of interest analysis using an SPM toolbox. In: Proceedings of the 8th International Conference on Functional Mapping of the Human Brain. Sendai, p. 497.
Brozzoli, C., Gentile, G., Ehrsson, H.H., 2012. That's near my hand! Parietal and premotor coding of hand-centered space contributes to localization and self-attribution of the hand. J. Neurosci. 32, 14573–14582.
Brozzoli, C., Gentile, G., Petkova, V.I., Ehrsson, H.H., 2011. FMRI adaptation reveals a cortical mechanism for the coding of space near the hand. J. Neurosci. 31, 9023–9031 the official journal of the Society for Neuroscience.
Brusa, F., Erden, M.S., Sedda, A., 2023. Influence of the somatic rubber hand illusion on maximum grip aperture. J. Mot. Behav. 55, 39–57.
Calhoun, V.D., Stevens, M.C., Pearlson, G.D., Kiehl, K.A., 2004. fMRI analysis with the general linear model: removal of latency-induced amplitude bias by incorporation of hemodynamic derivative terms. Neuroimage 22, 252–257.
Chancel, M., Ehrsson, H.H., Ma, W.J., 2022. Uncertainty-based inference of a common cause for body ownership. eLife 11, e77221.
Chen, T.L., Babiloni, C., Ferretti, A., Perrucci, M.G., Romani, G.L., Rossini, P.M., Tartaro, A., Del Gratta, C., 2008. Human secondary somatosensory cortex is involved in the processing of somatosensory rare stimuli: an fMRI study. Neuroimage 40, 1765–1771.
Coggan, D.D., Allen, L.A., Farrar, O.R., Gouws, A.D., Morland, A.B., Baker, D.H., Andrews, T.J., 2017. Differences in selectivity to natural images in early visual areas (V1–V3). Sci. Rep. 7, 2444.
Coppi, S., Jensen, K.B., Ehrsson, H.H., 2024. Eliciting the rubber hand illusion by the activation of nociceptive C and Adelta fibers. Pain 165 (10), 2240– 2256.
Corbetta, M., Kincade, J.M., Shulman, G.L., 2002. Neural systems for visual orienting and their relationships to spatial working memory. J. Cogn. Neurosci. 14, 508–523.
D'Alonzo, M., Mioli, A., Formica, D., Di Pino, G., 2020. Modulation of body representation impacts on efferent autonomic activity. J. Cogn. Neurosci. 32, 1104–1116.
D'Alonzo, M., Mioli, A., Formica, D., Vollero, L., Di Pino, G., 2019. Different level of virtualization of sight and touch produces the uncanny valley of avatar's hand embodiment. Sci. Rep. 9, 19030.
David, N., Fiori, F., Aglioti, S.M., 2014. Susceptibility to the rubber hand illusion does not tell the whole body-awareness story. Cogn. Affect. Behav. Neurosci. 14, 297–306.
De Castro, T.G., Barbosa Gomes, W., 2017. Rubber hand illusion: evidence for multisensory integration of proprioception. Av. Psicol. Latinoam. 35, 219–231.
Declaration of Helsinki, 2013. World Medical Association Declaration of Helsinki: ethical principles for medical research involving human subjects. Jama 310 (20), 2191–2194.
Downing, P.E., Jiang, Y., Shuman, M., Kanwisher, N., 2001. A cortical area selective for visual processing of the human body. Science 293, 2470–2473.
Ebisch, S.J., Perrucci, M.G., Ferretti, A., Del Gratta, C., Romani, G.L., Gallese, V., 2008. The sense of touch: embodied simulation in a visuotactile mirroring mechanism for observed animate or inanimate touch. J. Cogn. Neurosci. 20, 1611–1623.
Ehrsson, H., Wiech, K., Weiskopf, N., Dolan, R., Passingham, R., 2007a. Threatening a rubber hand that you feel is yours elicits a cortical anxiety response. Proc. Natl. Acad. Sci. U. S. A. 104, 9828–9833.
Ehrsson, H.H., 2007. The experimental induction of out-of-body experiences. Science 317, 1048.
Ehrsson, H.H., Holmes, N.P., Passingham, R.E., 2005. Touching a rubber hand: feeling of body ownership is associated with activity in multisensory brain areas. J. Neurosci. 25, 10564–10573.
Ehrsson, H.H., Spence, C., Passingham, R.E., 2004. That's my hand! Activity in premotor cortex reflects feeling of ownership of a limb. Science 305, 875–877.

Ehrsson, H.H., Wiech, K., Weiskopf, N., Dolan, R.J., Passingham, R.E., 2007b. Threatening a rubber hand that you feel is yours elicits a cortical anxiety response. Proc. Natl. Acad. Sci. U. S. A. 104, 9828–9833.
Ernst, M.O., Bülthoff, H.H., 2004. Merging the senses into a robust percept. Trends Cogn. Sci. 8, 162–169.
Fan, C., Coppi, S., Ehrsson, H.H., 2021. The supernumerary rubber hand illusion revisited: perceived duplication of limbs and visuotactile events. J. Exp. Psychol. Hum. Percept. Perform. 47, 810–829.
Fuchs, X., Riemer, M., Diers, M., Flor, H., Trojan, J., 2016. Perceptual drifts of real and artificial limbs in the rubber hand illusion. Sci. Rep. 6, 24362.
Gallagher, M., Colzi, C., Sedda, A., 2021. Dissociation of proprioceptive drift and feelings of ownership in the somatic rubber hand illusion. Acta Psychol. 212, 103192 (Amst).
Garbarini, F., Fossataro, C., Pia, L., Berti, A., 2020. What pathological embodiment/disembodiment tell us about body representations. Neuropsychologia 149, 107666.
Gassert, R., Moser, R., Burdet, E., Bleuler, H., 2006. MRI/fMRI-compatible robotic system with force feedback for interaction with human motion. IEEE ASME Trans. Mechatron. 11, 216–224.
Gentile, G., Bjornsdotter, M., Petkova, V.I., Abdulkarim, Z., Ehrsson, H.H., 2015. Patterns of neural activity in the human ventral premotor cortex reflect a whole-body multisensory percept. Neuroimage 109, 328–340.
Gentile, G., Petkova, V.I., Ehrsson, H.H., 2011. Integration of visual and tactile signals from the hand in the human brain: an FMRI study. J. Neurophysiol. 105, 910–922.
Giovaola, Y., Rojo Martinez, V., Ionta, S., 2022. Degraded vision affects mental representations of the body. Vis. Cogn. 30, 686–695.
Golaszewski, S., Frey, V., Thomschewski, A., Sebastianelli, L., Versace, V., Saltuari, L., Trinka, E., Nardone, R., 2021. Neural mechanisms underlying the Rubber Hand Illusion: a systematic review of related neurophysiological studies. Brain Behav. 11, e02124.
Guterstam, A., Gentile, G., Ehrsson, H.H., 2013. The invisible hand illusion: multisensory integration leads to the embodiment of a discrete volume of empty space. J. Cogn. Neurosci. 25, 1078–1099.
Haans, A., Kaiser, F.G., Bouwhuis, D.G., Ijsselsteijn, W.A., 2012. Individual differences in the rubber-hand illusion: predicting self-reports of people's personal experiences. Acta Psychol. 141, 169–177 (Amst).
Hagni, K., Eng, K., Hepp-Reymond, M.C., Holper, L., Keisker, B., Siekierka, E., Kiper, D. C., 2008. Observing virtual arms that you imagine are yours increases the galvanic skin response to an unexpected threat. PLoS One 3, e3082.
Heldmann, M., Spitta, G., Wagner-Altendorf, T., Munte, T.F., 2024. Threatening an illusory limb: an event-related potential study of the rubber hand illusion. Cogn. Behav. Neurol. 37, 99–106.
Henson, R., 2015. Analysis of variance (ANOVA). Brain Mapping: an Encyclopedic Reference. Elsevier, pp. 477–481.
Hornburger, H., Nguemeni, C., Odorfer, T., Zeller, D., 2019. Modulation of the rubber hand illusion by transcranial direct current stimulation over the contralateral somatosensory cortex. Neuropsychologia 131, 353–359.
Ionta, S., Heydrich, L., Lenggenhager, B., Mouthon, M., Fornari, E., Chapuis, D., Gassert, R., Blanke, O., 2011. Multisensory mechanisms in temporo-parietal cortex support self-location and first-person perspective. Neuron 70, 363–374.
Ionta, S., Martuzzi, R., Salomon, R., Blanke, O., 2014. The brain network reflecting bodily self-consciousness: a functional connectivity study. Soc. Cogn. Affect. Neurosci. 9, 1904–1913.
Ionta, S., Sforza, A., Funato, M., Blanke, O., 2013. Anatomically plausible illusory posture affects mental rotation of body parts. Cogn. Affect. Behav. Neurosci. 13, 197–209.
Jackson, P.L., Meltzoff, A.N., Decety, J., 2006. Neural circuits involved in imitation and perspective-taking. Neuroimage 31, 429–439.
Kalckert, A., Ehrsson, H.H., 2014a. The moving rubber hand illusion revisited: comparing movements and visuotactile stimulation to induce illusory ownership. Conscious. Cogn. 26, 117–132.
Kalckert, A., Ehrsson, H.H., 2014b. The spatial distance rule in the moving and classical rubber hand illusions. Conscious. Cogn. 30, 118–132.
Kammers, M.P., de Vignemont, F., Verhagen, L., Dijkerman, H.C., 2009. The rubber hand illusion in action. Neuropsychologia 47, 204–211.
Kanayama, N., Sato, A., Ohira, H., 2007. Crossmodal effect with rubber hand illusion and gamma-band activity. Psychophysiology 44, 392–402.
Kanayama, N., Sato, A., Ohira, H., 2009. The role of gamma band oscillations and synchrony on rubber hand illusion and crossmodal integration. Brain Cogn. 69, 19–29.
Kitada, R., Johnsrude, I.S., Kochiyama, T., Lederman, S.J., 2009. Functional specialization and convergence in the occipito-temporal cortex supporting haptic and visual identification of human faces and body parts: an fMRI study. J. Cogn. Neurosci. 21, 2027–2045.
Lesur, M.R., Weijs, M.L., Simon, C., Kannape, O.A., Lenggenhager, B., 2020. Psychometrics of disembodiment and its differential modulation by visuomotor and visuotactile mismatches. iScience 23 (3), 100901.
Limanowski, J., Blankenburg, F., 2015a. Network activity underlying the illusory self-attribution of a dummy arm. Hum. Brain Mapp. 36, 2284–2304.
Limanowski, J., Blankenburg, F., 2015b. Network activity underlying the illusory self-attribution of a dummy arm. Hum. Brain Mapp. 36, 2284–2304.
Limanowski, J., Lutti, A., Blankenburg, F., 2014a. The extrastriate body area is involved in illusory limb ownership. Neuroimage 86, 514–524.
Limanowski, J., Lutti, A., Blankenburg, F., 2014b. The extrastriate body area is involved in illusory limb ownership. Neuroimage 86, 514–534.
Longo, M.R., Cardozo, S., Haggard, P., 2008a. Visual enhancement of touch and the bodily self. Conscious. Cogn. 17, 1181–1191.
Longo, M.R., Schüür, F., Kammers, M.P., Tsakiris, M., Haggard, P., 2008b. What is embodiment? A psychometric approach. Cognition 107, 978–998.
Lush, P., Seth, A.K., Dienes, Z., 2021. Hypothesis awareness confounds asynchronous control conditions in indirect measures of the rubber hand illusion. R. Soc. Open Sci. 8, 210911.
Magnani, F.G., Cacciatore, M., Barbadoro, F., Ippoliti, C., Leonardi, M., 2024. Sense of ownership influence on tactile perception: is the predictive coding account valid for the somatic rubber hand Illusion? Conscious. Cogn. 123, 103710.
Martini, M., Kilteni, K., Maselli, A., Sanchez-Vives, M.V., 2015. The body fades away: investigating the effects of transparency of an embodied virtual body on pain threshold and body ownership. Sci. Rep. 5, 13948.
Matamala-Gomez, M., Gonzalez, A.M.D., Slater, M., Sanchez-Vives, M.V., 2019. Decreasing pain ratings in chronic arm pain through changing a virtual body: different strategies for different pain types. J. Pain 20, 685–697.
Matsumuro, M., Ma, N., Miura, Y., Shibata, F., Kimura, A., 2022. Top-down effect of body representation on pain perception. PLoS One 17, e0268618.
Moffatt, J., Finotti, G., Tsakiris, M., 2024. With hand on heart: a cardiac rubber hand illusion. Biol. Psychol. 186, 108756.
Naito, E., Roland, P.E., Ehrsson, H.H., 2002. I feel my hand moving: a new role of the primary motor cortex in somatic perception of limb movement. Neuron 36, 979–988.
Nilsson, M., Kalckert, A., 2021. Region-of-interest analysis approaches in neuroimaging studies of body ownership: an activation likelihood estimation meta-analysis. Eur. J. Neurosci. 54, 7974–7988.
Nurmi, T., Henriksson, L., Piitulainen, H., 2018. Optimization of proprioceptive stimulation frequency and movement range for fMRI. Front. Hum. Neurosci. 12, 477.
Okumura, K., Ora, H., Miyake, Y., 2020. Investigating the hand ownership illusion with two views merged in. Front. Robot. AI 7, 49.
Oldfield, R.C., 1971. The assessment and analysis of handedness: the Edinburgh inventory. Neuropsychologia 9, 97–113.
Pamplona, G., Gruaz, Q., Mauron, K., Ionta, S., 2022a. Abrupt visibility modifications affect specific subjective (not objective) aspects of body ownership. Acta Psychol. 229, 103672 (Amst).
Pamplona, G.S.P., Hardmeier, M., Younes, S., Goy, I., Fornari, E., Ionta, S., 2022b. Vision- and touch-dependent brain correlates of body-related mental processing. Cortex 157, 30–52.
Pamplona, G.S.P., Salgado, J.A.D., Staempfli, P., Seifritz, E., Gassert, R., Ionta, S., 2022c. Illusory body ownership affects the cortical response to vicarious somatosensation. Cereb. Cortex 32, 312–328.
Peelen, M.V., Downing, P.E., 2005. Selectivity for the human body in the fusiform gyrus. J. Neurophysiol. 93, 603–608.
Pyasik, M., Salatino, A., Burin, D., Berti, A., Ricci, R., Pia, L., 2019. Shared neurocognitive mechanisms of attenuating self-touch and illusory self-touch. Soc. Cogn. Affect. Neurosci. 14, 119–127.
Reinersmann, A., Landwehrt, J., Krumova, E.K., Peterburs, J., Ocklenburg, S., Gunturkun, O., Maier, C., 2013. The rubber hand illusion in complex regional pain syndrome: preserved ability to integrate a rubber hand indicates intact multisensory integration. Pain 154, 1519–1527.
Riemer, M., Kleinbohl, D., Holzl, R., Trojan, J., 2013. Action and perception in the rubber hand illusion. Exp. Brain Res. 229, 383–393.
Riemer, M., Trojan, J., Beauchamp, M., Fuchs, X., 2019. The rubber hand universe: on the impact of methodological differences in the rubber hand illusion. Neurosci. Biobehav. Rev. 104, 268–280.
Rohde, M., Di Luca, M., Ernst, M.O., 2011. The rubber hand illusion: feeling of ownership and proprioceptive drift do not go hand in hand. PLoS One 6, e21659.
Rotach, Z., Beazley, C., Ionta, S., 2024. Degraded visibility body-specifically affects mental rotation. Behav. Sci. 14, 784.
Sakamoto, M., Ifuku, H., 2021. Attenuation of sensory processing in the primary somatosensory cortex during rubber hand illusion. Sci. Rep. 11, 7329.
Schaefer, M., Heinze, H.J., Rotte, M., 2009. My third arm: shifts in topography of the somatosensory homunculus predict feeling of an artificial supernumerary arm. Hum. Brain Mapp. 30, 1413–1420.
Schröder, P., Schmidt, T.T., Blankenburg, F., 2019. Neural basis of somatosensory target detection independent of uncertainty, relevance, and reports. eLife 8, e43410.
Schwarzlose, R.F., Baker, C.I., Kanwisher, N., 2005. Separate face and body selectivity on the fusiform gyrus. J. Neurosci. 25, 11055–11059.
Serino, A., Alsmith, A., Costantini, M., Mandrigin, A., Tajadura-Jimenez, A., Lopez, C., 2013. Bodily ownership and self-location: components of bodily self-consciousness. Conscious. Cogn. 22, 1239–1252.
Shimada, S., Fukuda, K., Hiraki, K., 2009. Rubber hand illusion under delayed visual feedback. PLoS One 4, e6185.
Singer, T., Seymour, B., O'Doherty, J., Kaube, H., Dolan, R.J., Frith, C.D., 2004. Empathy for pain involves the affective but not sensory components of pain. Science 303, 1157–1162.
Tsakiris, M., 2010. My body in the brain: a neurocognitive model of body-ownership. Neuropsychologia 48, 703–712.
Tsakiris, M., Carpenter, L., James, D., Fotopoulou, A., 2010. Hands only illusion: multisensory integration elicits sense of ownership for body parts but not for non-corporeal objects. Exp. Brain Res. 204, 343–352.
Tsakiris, M., Haggard, P., 2005. The rubber hand illusion revisited: visuotactile integration and self-attribution. J. Exp. Psychol. Hum. Percept. Perform. 31, 80–91.
Tsakiris, M., Hesse, M.D., Boy, C., Haggard, P., Fink, G.R., 2007. Neural signatures of body ownership: a sensory network for bodily self-consciousness. Cereb. Cortex 17, 2235–2244.
Urgesi, C., Berlucchi, G., Aglioti, S.M., 2004. Magnetic stimulation of extrastriate body area impairs visual processing of nonfacial body parts. Curr. Biol. 14, 2130–2134.

Yarkoni, T., Poldrack, R.A., Nichols, T.E., Van Essen, D.C., Wager, T.D., 2011. Large-scale automated synthesis of human functional neuroimaging data. Nat. Methods 8, 665–670.

Zeller, D., Litvak, V., Friston, K.J., Classen, J., 2015. Sensory processing and the rubber hand illusion–an evoked potentials study. J. Cogn. Neurosci. 27, 573–582.

Zopf, R., Williams, M.A., 2013. Preference for orientations commonly viewed for one's own hand in the anterior intraparietal cortex. PLoS One 8, e53812.